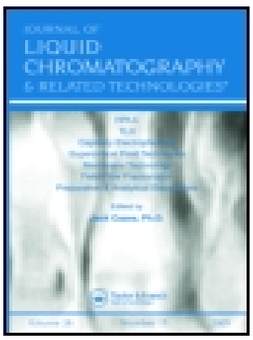

Taylor & Francis
Taylor & Francis Group

Journal of Liquid Chromatography & Related Technologies

ISSN: 1082-6076 (Print) 1520-572X (Online) Journal homepage: https://www.tandfonline.com/loi/ljlc20

Chemical profiling and quantification of Tanreqing injection, a systematic quality control strategy equipped with UPLC-Q-Orbitrap fusion MS

Su-Xiang Feng, Hao-Jie Zhang, Di Zhao, Rong-Rong Li, Xue-Hang Du, Pei-Yang Wang, Sheng-Nan Shu, Ling-Bo Qu & Jian-Sheng Li

To cite this article: Su-Xiang Feng, Hao-Jie Zhang, Di Zhao, Rong-Rong Li, Xue-Hang Du, Pei-Yang Wang, Sheng-Nan Shu, Ling-Bo Qu & Jian-Sheng Li (2020): Chemical profiling and quantification of Tanreqing injection, a systematic quality control strategy equipped with UPLC-Q-Orbitrap fusion MS, Journal of Liquid Chromatography & Related Technologies, DOI: 10.1080/10826076.2020.1723105

To link to this article: https://doi.org/10.1080/10826076.2020.1723105

JOURNAL OF LIQUID CHROMATOGRAPHY & RELATED TECHNOLOGIES
https://doi.org/10.1080/10826076.2020.1723105

Chemical profiling and quantification of Tanreqing injection, a systematic quality control strategy equipped with UPLC-Q-Orbitrap fusion MS

Su-Xiang Feng[a,b], Hao-Jie Zhang[a,b], Di Zhao[a,b], Rong-Rong Li[a,b], Xue-Hang Du[c], Pei-Yang Wang[a,b], Sheng-Nan Shu[a,b], Ling-Bo Qu[d], and Jian-Sheng Li[a,b]

[a]College of Pharmacy, Henan University of Traditional Chinese Medicine, Zhengzhou, Henan, China; [b]Co-construction Collaborative Innovation Center for Chinese Medicine and Respiratory Diseases, by Henan and Education Ministry of P. R., Zhengzhou, Henan, China; [c]Shanghai Kaibao Pharmaceutical Co. Ltd, Shanghai, China; [d]College of Chemistry and Molecular Engineering, Zhengzhou University, Zhengzhou, China

ABSTRACT

Tanreqing injection is a Chinese medical formula used to treatment of respiratory diseases. In our study, we developed a feasible and accurate strategy applying an ultra-high-performance liquid chromatography coupled with Q Exactive™ Plus-Orbitrap Fusion mass spectrometers (UPLC-Q-Orbitrap Fusion MS/MS) to clarify and quantify the chemical profiling of Tanreqing injection rapidly. A total of 80 ingredients were identified by comparing the accurate mass, fragment ions, and cleavage pathways, including flavonoids, phenyl propionic acid, coumarins, amino acids, cholesterol, etc. And 18 characteristic components among them were definitely identified by comparison with reference substance. Meanwhile, the 18 representative constituents were simultaneously measured in eight batches Tanreqing injection utilizing UPLC-Q-Orbitrap Fusion MS/MS in negative ion mode. Among the 18 components, beta-d-glucopyranosiduronic acid, baicalin, ursodeoxycholic acid, and chenodeoxycholic acid were the predominant constituents. In principal components analysis results, five dominating components were extracted, and the variant contribution rates were ranked as: 37.86, 22.86, 16.42, 9.80, 7.32%, with the accumulated value 94.26%. 5-caffeoylquinic acid, isochlorogenic acid C, and baicalin possessed larger loads on the first factor. Our research carried out qualitative and quantitative analysis on Tanreqing injection, provided a certain reference for the research on pharmacodynamic material basis and the selection of quality markers.

KEYWORDS

Qualitative; quantitative analysis; Tanreqing injection; UPLC-Q-Orbitrap fusion MS/MS

GRAPHICAL ABSTRACT

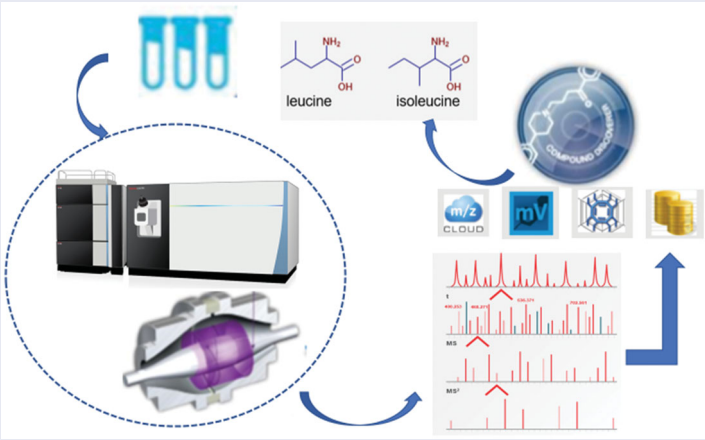

Introduction

At presently, Chinese medicine injection (CMI)[1–3] has been increasingly used in clinical practice as a rapid-acting modern dosage form. However, the safety and effectiveness of CMI are facing great challenges due to many potential elements including individual differences, drugs, pharmaceutical excipients, solvents, and syndrome differentiation that may cause adverse reactions[4–6] of CMI, and the biggest obstacle is the ambiguity in pharmacological basis of CMI. The complex acted pathways and mechanisms of

CONTACT Su-Xiang Feng fengsx221@163.com; Jian-Sheng Li li_js8@163.com Co-construction Collaborative Innovation Center for Chinese Medicine and Respiratory Diseases by Henan and Education Ministry of P. R., Zhengzhou, Henan 450046, China

Supplemental data for this article can be accessed on the publisher's website.

Chinese medicine formula (CMF) make it hard to interpret the chemical composition of Chinese medicine which exert its pharmacodynamic effect and it is difficult to explain the mechanism and characteristics because the uncertainty of chemical composition in CMF.[7–9] Therefore, the unknown chemical profile and quantitative analysis of CMF are of great significance for elucidating the clinical efficacy and active mechanism of the drug, establishing quality control strategies,[10] and solving the safety of CMI.

Tanreqing injection (TRQI), a heating-clearing and treating inflammation CMI is comprised of *Astragalus, Bear Bile Powder, Goat Horn, Honeysuckle, and Forsythia.* Clinically, TRQI showed a significant effect on the treatment of acute pneumonia and presented a good therapeutic effect on upper respiratory tract infection and viral pneumonia.[11,12] In addition, TRQI also adhere with unique effects[13,14] on the treatment of childhood pneumonia, hepatitis, and cholecystitis. Nowadays, the instruments commonly applied for the identification and determination of chemical constituents of Chinese medicine include high-performance liquid chromatography (HPLC), ultra-high performance liquid phase (UPLC), high performance liquid chromatography-mass spectrometry (HPLC-MS).

Referring the previous literatures,[15–18] the sensitivity of HPLC is generally poor and usually only respond to higher levels of components, while the finer size particle size and higher sensitivity of UPLC making the separation of components more complete and faster. In additional, some characteristic components with weak ultraviolet (UV) absorption are easily ignored as the detection principle of HPLC and UPLC are the ultraviolet absorption by components. In contrast, mass spectrometry detects compounds based on molecular weight, independent of the UV absorption of the component. In summary, the UPLC-MS overcome the shortcomings of HPLC and UPLC, such as: low sensitivity, narrow detection ranges, and long analysis time when conduct quantitative identification and qualitative analysis of TRQI. In previous studies, Liu et al.,[19] developed a liquid chromatography-diode array detector (DAD) coupled with electrospray ionization time-of-flight mass spectrometry (ESI-TOF/MS) for the screening and identification of the multiple components in Tanreqing injection and 12 components were explicitly identified, Sun et al.,[20] established a method proposed high performance liquid chromatography coupled with photodiode array detection and evaporative light scattering detection (HPLC-DAD-ELSD) and identified 53 compounds on a formula database of 515 known compounds with the assistance of accurate mass measurement for molecular ions and characteristic fragment ions. However, UPLC-Orbitrap MS featured higher resolution, faster polarity switching functions, wider detected mass range and more chemical compositions than Q-TOF-MS.[21,22]

In our research, UPLC-Q-Orbitrap Fusion MS/MS was selected for characterizing the overall compositions of TRQI and measured the contents of the characteristic components. The components in TRQI entered the mass spectrometer through an electrospray ionization interface. In qualitative analysis, the structure of the substance was estimated based on the accurate molecular mass and the cleavage pathway measured by UPLC-Q-Orbitrap Fusion MS/MS, and compared with m/z cloud library and other literatures. In total, 80 unknown constituents were identified including flavonoids, phenyl propionic acid, coumarins, amino acids, cholesterol, etc. and 18 major components among them were explicitly identified by comparing with the retention time and accurate mass with reference substance. Our investigation was the first time to characterize the panoramic chemical composition of TRQI and determine the multi-composition content in several batches of TRQI.

Experiment

Materials and chemicals

TRQI samples were produced by Shanghai Kai Bao Pharmaceutical Co. Ltd. (Shanghai, China). The reference standards: beta-d-glucopyranosiduronic acid, chlorogenic acid, 5-caffeoylquinic acid, 4-dicaffeoylquinic acid, forsythoside A, 3,4-dicaffeoylquinic acid, scutellarin, luteoloside, isochlorogenic acid A, isochlorogenic acid C, baicalin, baicalein, phillyrin, wogonin, taurochenodeoxycholic acid, 3α,7α,12α-trihydroxy-5beta-cholanic acid, ursodeoxycholic acid, chenodeoxycholic acid and puerarin (internal standard, IS) were purchased from the National Institute for Food and Drug Control (Beijing, China). The purity of all the reference substances was higher than 98% determined by HPLC analysis and their chemical structures were displayed in Figure 1. HPLC grade of acetonitrile, methanol, and formic acid were provided by Fisher Scientific (Fair Lawn, NJ, USA). Formic acid was obtained from Fisher Scientific ((Fair Lawn, NJ07410, USA). And, the other solvents, obtained from Fuyu Chemical Co., Ltd. (Tianjin, China) were of analytical grade. Ultra-water was prepared using a Milli-Q system (Millipore, Bedford, USA). Eight batches of TRQI were purchased from Shanghai Kai Bao Pharmaceutical Co. Ltd. (Shanghai, China) and their batch numbers were 1809203, 1806211, 1806208, 1807209, 1805210, 1809206, 1807215, and 1812208, respectively.

Preparation of standard solutions and samples

The methanol solutions containing 0.3200 mg mL^{-1} beta-d-glucopyranosiduronic acid, 0.1900 mg mL^{-1} chlorogenic acid, 0.2010 mg mL^{-1} 5-caffeoylquinic acid, 0.1370 mg mL^{-1} 4-dicaffeoylquinic acid, 0.2100 mg mL^{-1} forsythoside A, 0.1820 mg mL^{-1} 3,4-dicaffeoylquinic acid, 0.1395 mg mL^{-1} scutellarin, 0.1705 mg mL^{-1} luteoloside, 0.2720 mg mL^{-1} isochlorogenic acid A, 0.2520 mg mL^{-1} isochlorogenic acid C, 0.1355 mg mL^{-1} baicalin, 0.4240 mg mL^{-1} baicalein, 0.1950 mg mL^{-1} phillyrin, 0.2350 mg mL^{-1} wogonin, 0.1930 mg mL^{-1} taurochenodeoxycholic acid, 0.1880 mg mL^{-1} 3α,7α,12α-Trihydroxy-5beta-cholanic acid, 0.2000 mg mL^{-1} ursodeoxycholic acid and 0.0876 mg mL^{-1} chenodeoxycholic acid were prepared and stored in refrigerator at 4 °C. These reference solutions were diluted with methanol to appropriate concentration range for qualitative analysis and calibration

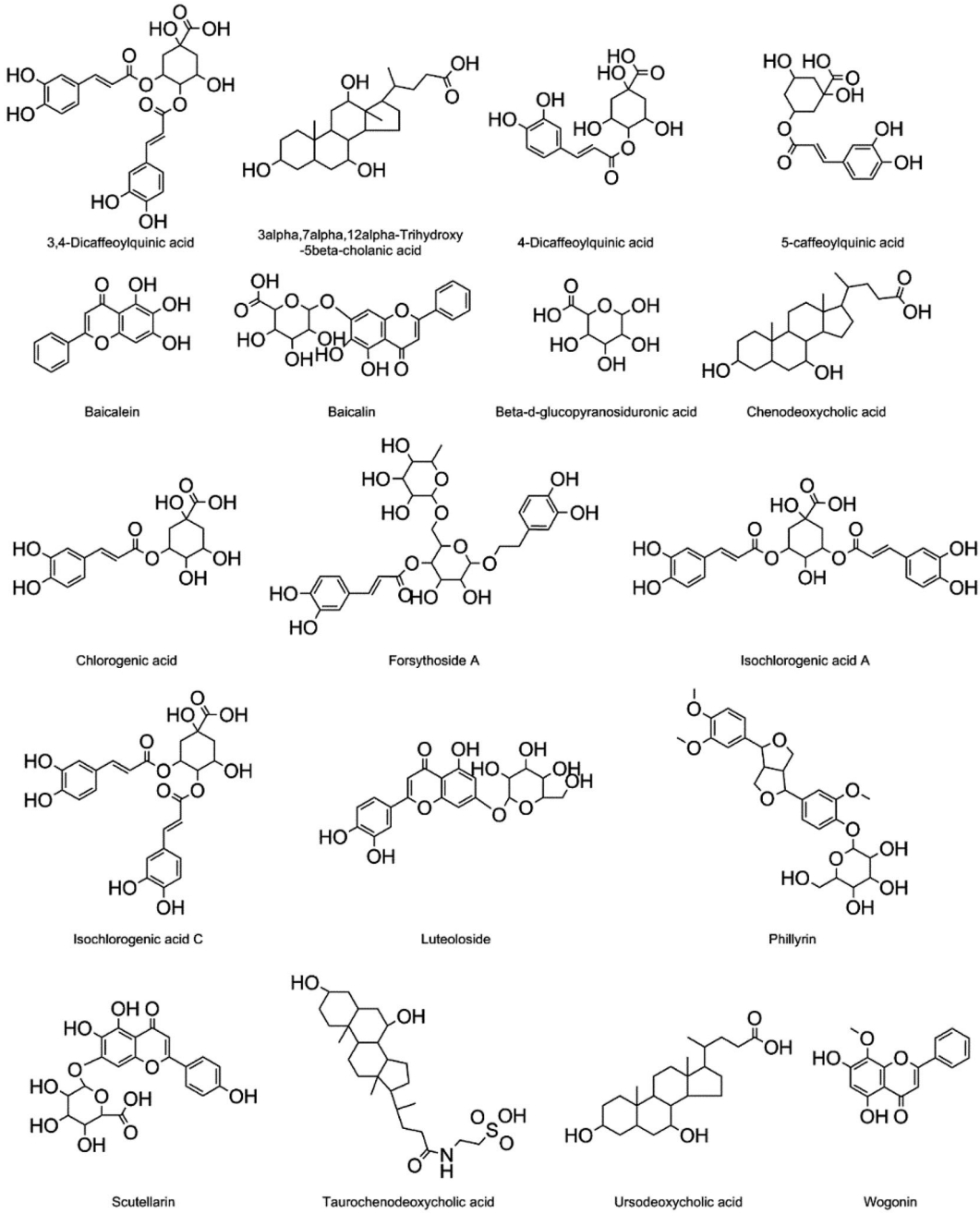

Figure 1. The chemical structure of 18 components determined in quantitative analysis.

curves were established in triplicate. The eight batches of TRQI were diluted to appropriate concentration with methanol.

In the preparation of sample TRQI, the sample TRQI were diluted at the ratio of 1:100 (v:v) with methanol. The mixture was vortexed, centrifuged at 6000 r/min for 10 min, and then the supernatant was taken for analysis. All the solutions and extraction obtained were filtered through 0.22 μm pore size filters and were stored at −20 °C before analysis.

Chromatographic and mass spectrometric condition

Chromatographic separation was performed on an Ultimate 3000 UPLC system (Thermo Scientific, USA) equipped with an on-line degasser, a quaternary pump, an autosampler and a column temperature compartment. The process was carried out on an Accucore^{TM} C_{18} column (2.1 mm × 100 mm, 1.9 μm) (Waters Co. Ltd., USA). A heated electrospray ionization (HESI) ion source was used for the ionization of target compounds. Data acquisition, peak integration, and calibration were performed using Xcalibur®3.0 software and data analysis were performed using Compound Discoverer 3.0 and Mass Frontier 7.0.

In qualitative analysis, the mobile phase for chromatographic separation comprised of 0.1% (v:v) aqueous formic acid in water (A) and methanol (B) and the gradient elution were as follows: 0–5 min, 10–45% B; 5–13 min, 45–65% B; 13–18 min, 65–82% B; 18–27 min, 82–97% B. The column temperature was set at 30 °C with a flow rate of

Table 1. The relevant MS parameter of the 18 measured constituents.

Analyte	$[M–H]^-$ (*m/z*)	Retention time (min)
Beta-d-glucopyranosiduronic acid	193.0342	1.28
Chlorogenic acid	353.0867	4.36
5-caffeoylquinic acid	353.0867	6.63
4-Dicaffeoylquinic acid	353.0867	7.32
Forsythoside A	623.197	12.32
3,4-Dicaffeoylquinic acid	515.1184	12.4
Scutellarin	461.0714	12.44
Luteoloside	447.0921	12.5
Isochlorogenic acid A	515.1184	13.79
Isochlorogenic acid C	515.1184	15.41
Baicalin	445.0765	15.15
Baicalein	269.0444	17.91
Phillyrin	533.2017	23.21
Wogonin	283.06	18.97
Taurochenodeoxycholic acid	498.2883	20.59
3α,7α,12α-Trihydroxy-5beta-cholanic acid	407.2792	21.68
Ursodeoxycholic acid	391.2842	21.03
Chenodeoxycholic acid	391.2842	22.77

0.3 mL min^{-1}. The injection volume was set as 5 μL. The Q-Orbitrap mass spectrometer was carried out in the full scan mode and the quality range from 100 to 1000 *m/z* with the resolution of 120,000. The optimized parameters of MS are follows: spray voltage: +3.5 KV or −2.5 KV under positive and negative mode; capillary temperature: 350 °C, auxiliary gas heater temperature: 300 °C; capillary voltage: 4 KV, sheath gas flow rate: 35 arbitrary units (a.u.); auxiliary gas flow rate: 5 a.u.; sweep gas flow rate: 0 (a.u.). Nitrogen was used as nebulizing and dry gas. In additional, the automatic gain control (AGC) target was maintained at 4.0 e^5 and the maximum injection time (IT) was 50 ms. In order to narrow down the options, elements in use was set as C 0–40, H 0–70, O 0–20, Na 0–1 and mass tolerance defined as <10 ppm in the molecular analysis.

The gradient elution performed in the quantitative analysis was as following condition: 0–7 min, 10–39% B; 7–17 min, 39–52% B; 17–18 min, 52–70% B; 18–25 min, 70–90% B. The flow rate was 0.2 mL min^{-1}. The ESI source was in negative ionization mode and spray voltage was set as −3.5 V. The relevant MS parameter of the 18 measured constituents was shown in Table 1.

Results and discussion

Optimization of UPLC and MS condition

In the experiment, formic acid was added to the mobile phase to improve peak shape and increase ionization efficiency. And we compared three different concentrations of formic acid water (0.05, 0.1, and 0.2%) and found that the peak shape was improved significantly at higher concentrations. However, considering that high concentration of formic acid may cause the negative ion mode response to be suppressed we determined 0.1% formic acid in water as mobile phase solvent A. And the influence of flow rate (0.2 mL min^{-1}, 0.3 mL min^{-1}, and 0.4 mL min^{-1}) on relative abundance and resolution was investigated. The results showed that 0.4 mL min^{-1} flow rate would lower sensitivity due to discharge formed by solvent accumulated at ionization area. So, flow rate of 0.2 mL min^{-1} was optimized for quantitative analysis. In order to make the separation of the components in TRQI more complete while a higher flow rate of 0.3 mL min^{-1} was set for qualitative identification to reduce the running time. In term of MS condition, ESI (electrospray ionization) provided better sensitivity than APCI (atmospheric pressure chemical ionization). And parameters such as gas flow, capillary voltage, cone voltage were optimized to obtain the highest signal response of ion. In addition, the negative ion detection mode showed better sensitivity than the positive ion detection mode in quantitative analysis.

Qualitative analysis of TRQI

A UHPLC–Q-Orbitrap Mass Spectrometer, an instrument with high sensitivity and accuracy was employed to identify the total composition contained in TRQI. The analysis processions were as follows: firstly, the relative molecular mass was estimated by using the Compound Discovered 3.0 software; secondly, the fracture mode and related literature were reviewed; finally, the chemical structure and the cleavage pathway were further determined by Thermo Scientific™ Mass Frontier 7.0 software. The total ion chromatogram (TIC) of TRQI were shown in Figure 2, including positive mode and negative mode. In this study, chemical structures of 80 unknown compounds were analyzed, including 9 flavonoids, 14 phenylpropanoids, 20 amino acids and alkaloids, 4 bile acids and 33 other compounds. Eighteen of these compounds were completely confirmed by comparing the retention time and mass spectral data of the control and unknown components. In addition, based on the chemical components contained in the various herbs comprised of TRQI, we assigned the ingredients to the 80 components. It was speculated that flavonoids were mainly derived from *Scutellaria baicalensis*[23–25] and *Fructus forsythia.*[26,27] However, since TRQI does not contain Scutellaria baicalensis but only baicalin was added, baicalein and scutellarin may be converted from baicalin during the preparation of TRQI. Phenylpropanoids are a general summary of phenylpropionic acids, coumarins and lignans. Most of the phenylpropanoids in TRQI were derived from Honeysuckle,[28,29] such as chlorogenic acid and isochlorogenic acid C. Their quantitative determination in TRQI (batches 1806211) resulted in 246.10 and 373.66 ng/mL, respectively. Bear bile powder[30,31] was the source of bile acids while Cornu gorais[32,33] was the main source of amino acids and alkaloids.

Identification of unknown components in negative ion mode

Thirty unknown components were identified in negative ion mode and listed in Table 2. In the MS/MS experiment of beta-d-glucopyranosiduronic acid (NO.1, t_R=0.94 min), the major fragments at *m/z* 113.02412 indicated the loss of CO group from the precursor ion $[M–H]^-$. The MS/MS spectrum of NO.3 (t_R=3.14 min) and NO.4 (t_R=4.14 min) were shown in the Figure 3. In MS/MS spectra, the base peaks of chlorogenic acid and 5-caffeoylquinic acid were $[M–H–C_9H_6O_3]^-$ ion at *m/z* 191.05582 and 191.05568,

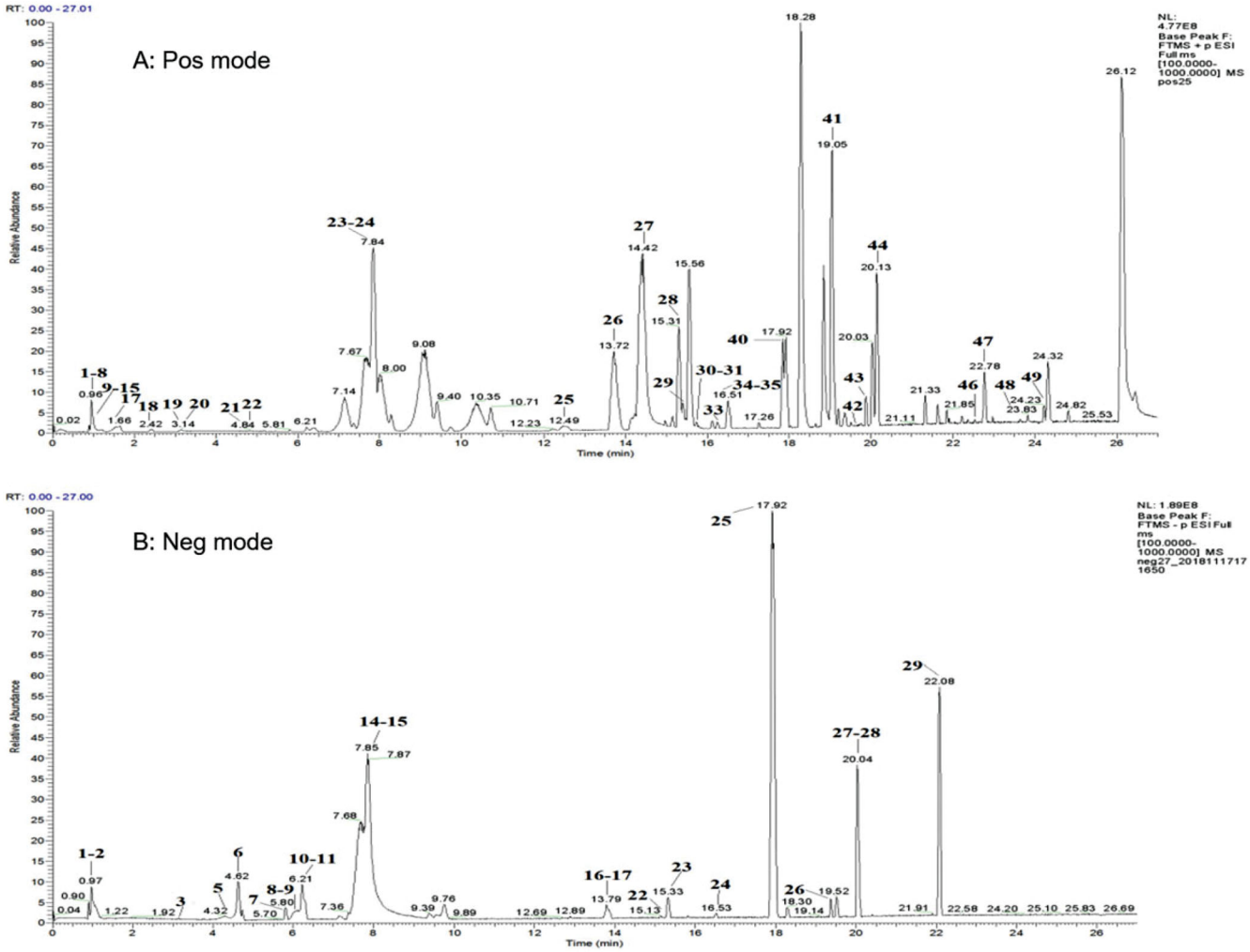

Figure 2. The total ion chromatogram (TIC) of TRQI.

respectively, and the further splitting of H_2O and CH_2O were discovered. Chlorogenic acid and 5-caffeoylquinic acid were stereo-isomerized and showed same cleavage mode. Chlorogenic acid (NO.3, $t_R = 3.14$ min), 5-caffeoylquinic acid and 4-dicaffeoylquinic acid (NO.5, $t_R = 4.36$ min) all have a quinic acid ($C_7H_{12}O_6$) structure and are isomers for the same relative molecular mass and pyrolysis ion $C_7O_5H_9^-$, $C_9O_3H_6^-$, $C_8O_2H_7^-$. According to the cleavage of NO.9 ($t_R = 6.08$ min), ions at *m/z* 353.08774, 179.03456, 173.04520, 161.02460, 135.04477 were discovered, resulting that NO.9 was identified as 3,4-dicaffeoylquinic acid and the retention time and accurate molecular mass of reference proved our speculation. Combined with the literatures,[28,29] NO.12 which possessed the same skeleton with NO.9 were assigned as isochlorogenic acid A ($t_R = 6.77$ min). In addition, isochlorogenic acid C (NO.13, $t_R = 7.01$ min) were confirmed by comparing with the retention time of reference substance. NO.10 (t_R=6.28 min) gave the $[M+H-Glu]^-$ ion at *m/z* 287.05466 and Glu^- ion at *m/z* 175.02417 which suggest the presence of the glycoside unit in the structure and NO.10 was tentatively assigned as Scutellarin by comparing with reference substance. No.15 (t_R = 7.88 min) gave $[M-H]^-$ ion at *m/z* 269.04555 ($C_{15}H_9O_5^-$) in the full scan mass spectrum with the characteristic fragment ions at *m/z* 241.05003 ($C_{14}H_9O_4^-$) which was attributed to the loss of the CO unit (28 Da). By comparing with retention time and high-resolution accurate mass of reference standards, NO.19 (t_R=14.11 min) was identified as wogonin. NO.19 and NO.20 (t_R=14.11 min) gave the same *m/z* and the accurate mass, thus NO.20 was speculated as wogonin isomer. Cholic acid components often exhibit strong acidity due to the presence of carboxyl groups. The cracking process often loses a hydrogen ion and exhibits a quasi-ion peak as the base peak. For example, taurochenodeoxycholic acid (NO. 21, t_R=14.99 min), ursodeoxycholic acid (NO. 25, t_R=17.96 min) displayed $[M-H]^-$ at *m/z* 498.28909 and *m/z* 391.28494, respectively. Of course, the elimination of the neutral group HCOOH and H_2O (18 Da) were also cleavage ways of the cholic acid components. 3α,7α, 12α-trihydroxy-5beta-cholanic acid (NO. 22, t_R=15.14 min) showed the diagnostic loss of the H (1 Da) with the ion at *m/z* 407.28030, and the further elimination of HCOOH unit at *m/z* 361.27414, while chenodeoxycholic acid (NO. 27, t_R=20.06 min) gave the characteristic fragment ion $[M-H-H_2O]^-$ at *m/z* 373.27402.

Taking into account the sources of these 30 unknown ingredients, the corresponding components in negative ion mode are mostly derived from honeysuckle and bear bile

Table 2. Thirty unknown components were identified in negative ion mode.

No.	Compounds	t_R (min)	Formula	Sources	Ion Mode	Experimental MS (*m/z*)	Measured MS (*m/z*)	Delta (ppm)	NL	HPLC-ESI-MS/MS (*m/z*)
1	Beta-d-glucopyranosiduronic acid	0.94	$C_6H_{10}O_7$	H	–	193.03522	193.03538	4.874	4.81E6	**113.02412**,101.02417
2	Quinic acid	1.00	$C_7H_{12}O_6$	H	–	191.05580	191.05611	4.111	1.02E7	**191.05580**,173.04532,171.02962,143.03551
3	Chlorogenic acid	3.14	$C_{16}H_{18}O_9$	H	–	353.08781	353.08781	3.120	2.48E6	**191.05582**,173.04584,161.02399,135.04488
4	5-caffeoylquinic acid	4.14	$C_{16}H_{18}O_9$	H	–	353.08783	353.08781	3.176	2.28E6	**191.05568**,173.04504,161.02393,135.04520
5	4-Dicaffeoylquinic acid	4.36	$C_{16}H_{18}O_9$	H	–	353.08775	353.08781	2.950	2.35E6	**179.03465**,173.04520,161.02457,135.04477
6	2-Methylbenzoic acid	4.62	$C_8H_8O_2$	H	–	135.04407	135.04515	0.104	1.76E7	**135.0474**,107.04955,92.02629
7	Methy 1-(hexopyranosyloxy)-5-hydroxy-7-(hydroxymethyl)-1,4a,5,7a-tetrahydrocyclopenta(c)pyran-4-carboxylate	5.81	$C_{17}H_{24}O_{11}$	NO	–	403.12445	403.12458	2.387	6.29E6	371.09869
8	Forsythoside A	6.00	$C_{29}H_{36}O_{15}$	F	–	623.19791	623.19814	1.385	9.80E4	179.03467, **161.02403**,135.04506
9	3,4-Dicaffeoylquinic acid	6.08	$C_{25}H_{24}O_{12}$	H	–	515.11942	515.11950	1.975	4.47E6	353.08774,179.03456,**173.04520**,161.02460,135.04477
10	Scutellarin	6.28	$C_{21}H_{18}O_{12}$	S	−/+	461.0718/463.08658	461.07255/463.08710	0.754/-1.128	1.81E6/2.24E6	**(-)175.02417/287.05466(+)**
11	Luteoloside	6.29	$C_{21}H_{20}O_{11}$	H	–	447.09304	447.09328	1.906	9.74E6	284.03238
12	Isochlorogenic acid A	6.77	$C_{25}H_{24}O_{12}$	H	–	515.11947	515.11950	2.072	1.82E6	353.08697,191.05550,179.03453,**173.04506**,135.04471
13	Isochlorogenic acid C	7.01	$C_{25}H_{24}O_{12}$	H	–	515.11945	515.11950	2.034	1.67E6	515.11950
14	Baicalin	7.82	$C_{21}H_{18}O_{11}$	S	−/+	445.07781/447.09247	445.07763/447.09219	2.859/0.631	2.13E8/2.01E8	**(-)311.05679/271.05975(+)**
15	Baicalein	7.88	$C_{15}H_{10}O_5$	S	–	269.04552	269.04555	3.978	7.31E7	**269.04517,241**.05003
16	Butylparaben	13.80	$C_{11}H_{14}O_3$	H	–	193.08650	193.08702	3.000	6.98E6	**193.08650**
17	Phillyrin	13.82	$C_{27}H_{34}O_{11}$	F	–	533.20225	533.20284	0.960	7.17E6	NO
18	2,2-Diethoxy-1-phenylethanon	14.00	$C_{12}H_{16}O_3$	F	–	207.10254	207.10267	4.680	2.13E6	207.10229
19	Wogonin	14.11	$C_{16}H_{12}O_5$	S	–	285.07564	285.07575	−0.386	2.80E6	270.05176,253.04878
20	Wogonin isomer	14.54	$C_{16}H_{12}O_5$	S	–	285.07576	285.07575	0.035	9.57E5	270.05197
21	Taurochenodeoxycholic acid	14.99	$C_{26}H_{45}NO_6S$	B	–	498.28887	498.28948	0.973	2.41E6	**498.28909**
22	3α,7α,12α-Trihydroxy-5beta-cholanic acid	15.14	$C_{24}H_{40}O_5$	B	–	407.28004	407.28030	2.061	3.21E6	**407.27976**,361.27414
23	Botrydial	15.38	$C_{17}H_{26}O_5$	NO	–	309.17076	309.17075	3.589	6363E6	**309.17059**
24	Gingerol	16.56	$C_{17}H_{26}O_4$	H	–	293.17575	293.17583	3.460	4.11E6	293.17535
25	Ursodeoxycholic acid	17.96	$C_{24}H_{40}O_4$	B	–	391.28564	391.28538	3.460	1.73E8	**391.28494**
26	Antroquinonol A	19.41	$C_{24}H_{38}O_4$	NO	–	389.26922	389.26973	1.500	8.63E6	**389.26947**
27	Chenodeoxycholic acid	20.06	$C_{24}H_{40}O_4$	B	–	391.28560	391.28538	3.358	6.57E7	**373.27402**
28	Dodecyl sulfate	20.08	$C_{12}H_{26}O_4S$	B	–	265.14780	265.14790	3.747	4.95E7	86.11295
29	2,2′-Methylenebis(4-methyl-6-tert-butylphenol)	22.07	$C_{23}H_{32}O_2$	NO	–	339.23301	339.23295	3.400	9.63E7	**339.23267**
30	4-Dodecylbenzenesulfonic acid	22.49	$C_{18}H_{30}O_3S$	B	–	325.18456	325.18429	4.207	3.36E6	**325.18375**

Bold character: the base peak in MS/MS spectra. *Abbreviation*: Bear gallbladders powder (B); Honeysuckle (H); *Fructus forsythia* (F): *Scutellaria baicalensis* (B); No known (NO).

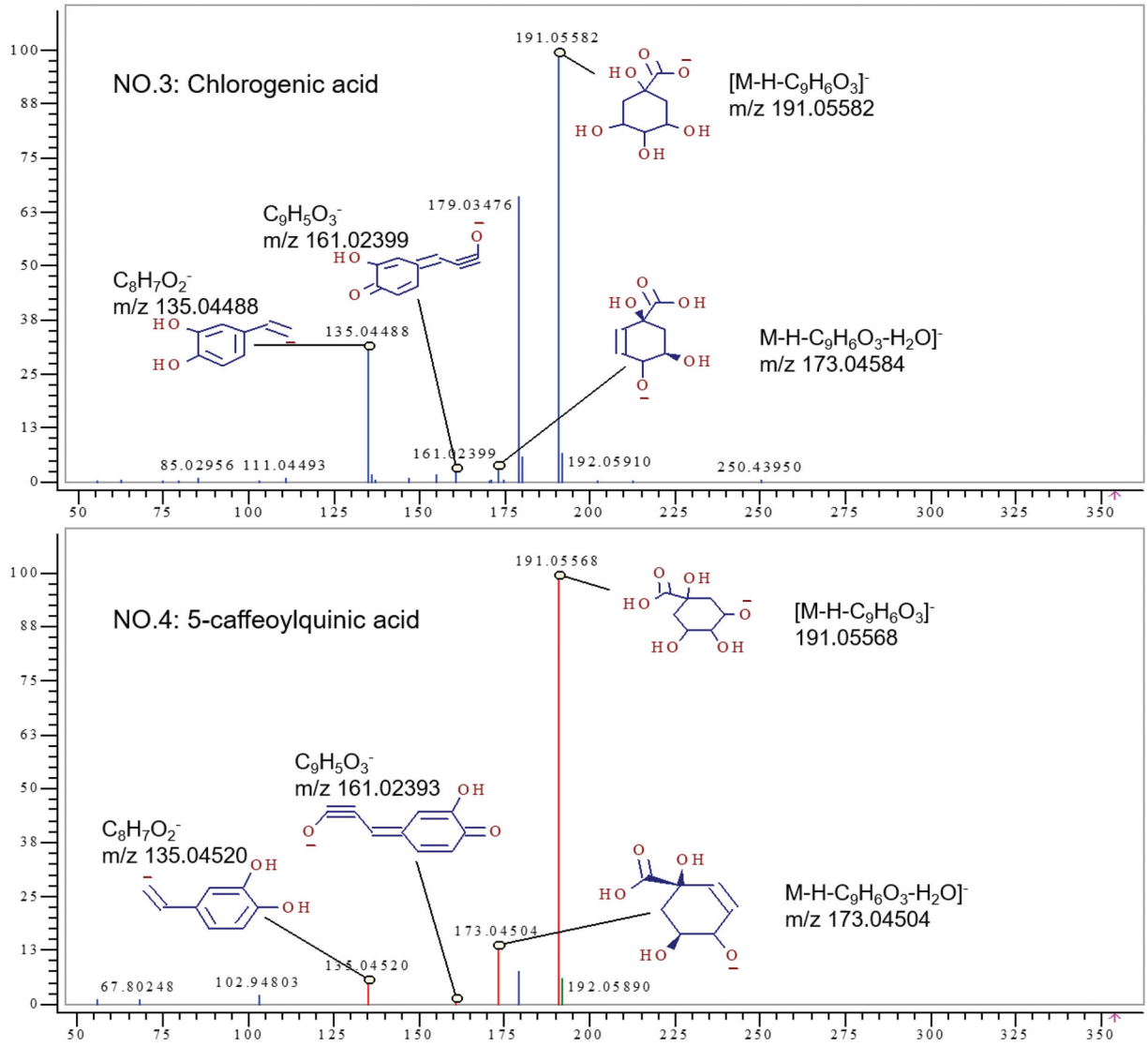

Figure 3. The MS/MS spectrum of chlorogenic acid and 5-caffeoylquinic acid.

powder. Quinic acid, chlorogenic acid, 5-caffeoylquinic acid, 4-dicaffeoylquinic acid, 3,4-dicaffeoylquinic acid, isochlorogenic acid A, and their isomer were derived from honeysuckle,[29,34] so conjectured that the organic acid components in honeysuckle were basic substances in TRQI that played a pharmacodynamic role in treatment. After all, a large number of studies have shown that organic acid components in honeysuckle presented antioxidant effects and enhanced the body's immune function. As botanical research discovered, taurochenodeoxycholic acid, 3α,7α, 12α-trihydroxy-5beta-cholanic acid, ursodeoxycholic acid and chenodeoxycholic acid were from bear bile powder,[30,31] and quantitative analysis results in this study showed that ursodeoxycholic acid and Chenodeoxycholic acid were the principal components in TRQI.

Identification of unknown components in positive ion mode

The detailed MS data of 50 unknown constituents detected and deduced in positive mode were list in Table 3. From previous studies, it was concluded that peptides, amino acids, phospholipids, and other nitrogen-containing components were the main components in goat horns. In this study, 13 species of amino acids and 7 other nitrogen-containing components were successfully identified. Amino acids usually have a carboxyl group and an amino group on the same carbon atom, and they tend to lose the neutral molecules HCOOH (46 Da) and NH3 (17 Da) during cleavage.[32] The formation of the base peak is often attributed to the absence of HCOOH unit from the quasi-molecular ion $[M+H]^+$. For example, the base peak of leucine and isoleucine were expressed as $[M+H–HCOOH]^+$. In the MS/MS2 spectra of NO. 8 (t_R=0.97 min) and NO. 17 (t_R=1.63 min), fragment ions $[M+H–HCOOH]^+$ ($C_5H_{12}N^+$) at *m/z* 86.09652 and 86.09654, $[M+H–HCOOH–NH_3]^+$ ($C_5H_9^+$) at *m/z* 69.07001 and 69.07002, were obtained, therefore NO. 8 was speculated as Leucine. Due to the similar molecular structures and cracking laws, NO. 17 was further deduced as leucine isomer: isoleucine. NO. 2 (t_R=0.94 min) displayed $[M+H]^+$ ion at *m/z* 106.06987($C_3H_8NO_3^+$), and

Table 3. The detailed MS/MS data of 50 unknown constituents detected and deduced in positive mode.

No.	Compounds	t_R (min)	Formula	Sources	Ion Mode	Experimental MS (*m/z*)	Measured MS (*m/z*)	Delta (ppm)	NL	HPLC-ESI-MS/MS (*m/z*)
1	L-Arginine	0.92	C6H14N4O2	C	+	175.11897	175.11895	0.101	7.71E5	158.09326, 130.09749, 116.07090, 114.05488
2	D-serine	0.94	C3H7NO3	C	+	106.04982	106.04987	−0.468	2.51E7	88.03944, 60.04453
3	Aspartic acid	0.95	C4H7NO4	C	+	134.04487	134.04478	0.640	3.81E7	88.03908, 74.02367
4	Proline isomer	0.96	$C_5H_9NO_2$	C	+	116.07058	116.07061	−0.216	3.81E7	85.02845, 84.04451
5	4-Guanidinobutyric acid	0.96	$C_5H_{11}N_3O_2$	C	+	146.09235	146.09240	−0.364	3.81E7	128.08180, 104.07070, 87.04412, 86.06017, 60.05573
6	2-Acetylphenol	0.96	$C_8H_8O_2$	F	+	137.05962	137.05971	−0.628	2.46E6	136.05119, 119.04897, 94.04127, 91.05431
7	Valine	0.97	$C_5H_{11}NO_2$	C	+	118.08621	118.08626	−0.382	3.26E7	72.04456, 61.02849
8	Leucine	0.97	$C_6H_{13}NO_2$	C	+	132.10186	132.10191	−0.342	3.26E7	86.09652, 69.07001
9	Glutamic acid	0.99	$C_5H_9NO_4$	C	+	148.06040	148.06043	−0.232	9.23E6	130.04990,102.05504,84.04451
10	Proline	1.00	$C_5H_9NO_2$	C	+	116.07056	116.07061	−0.389	1.52E7	98.06017,88.07590,70.06526
11	Homoserine	1.00	$C_4H_9NO_3$	C	+	120.06558	120.06552	0.502	1.87E7	120.08079, 102.05499, 74.06014, 56.04962
12	Pyroglutamic acid	1.01	$C_5H_7NO_3$	C	+	130.04987	130.04987	0.003	3.12E6	84.04446
13	Pulegone	1.01	$C_{10}H_{16}O$	F	+	153.12745	153.12739	0.381	1.65E5	135.08046, 125.09651, 111.08058, 107.08521, 97.06476
14	Adenosine	1.02	$C_{10}H_{13}N_5O_4$	C	+	268.10408	268.10403	0.185	2.55E6	136.06168
15	2,4-Octadienal	1.07	$C_8H_{12}O$	F	+	125.09602	125.09609	−0.572	2.41E5	109.06490, 107.08566, 95.04921, 83.04933, 81.07001
16	Tyrosine	1.39	$C_9H_{11}NO_3$	C	+	182.08116	182.08117	−0.054	2.34E6	165.05426, 136.07567, 123.04405, 119.04916
17	Isoleucine	1.63	$C_6H_{13}NO_2$	C	+	132.10184	132.10191	−0.494	7.99E6	86.09654, 69.07002
18	L-Phenylalanine	2.38	C9H11NO2	C	+	166.08633	166.08626	0.451	3.34E6	120.08083
19	N2-(tert-Butoxycarbonyl)-L-leucinamide	2.90	$C_{11}H_{22}N_2O_3$	C	+	231.17052	231.17032	0.869	2.08E6	118.08628, 86.09649
20	N2-(tert-Butoxycarbonyl)-L-leucinamide	3.21	$C_{11}H_{22}N_2O_3$	C	+	231.17055	231.17032	0.999	2.76E6	132.10184, 118.08622, 86.09654
21	Caffeic acid	4.6	$C_9H_8O_4$	F	+	181.04936	181.04954	−0.968	2.54E6	163.03886, 149.02321, 145.02830, 135.04405, 117.03352
22	3-Methyl-2H-furo(2,3-c) pyran-2-one	4.75	$C_8H_6O_3$	C	+	151.03893	151.03897	−0.269	2.22E6	123.04387, 107.04887, 95.04926
23	Genistein	7.82	$C_{15}H_{10}O_5$	F# H	+	271.06014	271.06010	0.148	2.13E8	253.04889
24	Coumestrol	7.84	$C_{15}H_8O_5$	F	+	269.04423	269.04445	−0.817	2.16E8	253.04889, 225.05428
25	Diethyl phthalate	12.49	$C_{12}H_{14}O_4$	NO	+	223.09670	223.09648	0.962	8.30E6	167.03365, 149.02316
26	Glycitein	13.75	$C_{16}H_{12}O_5$	F	+	285.07585	285.07575	0.351	1.54E7	270.05188, 253.05019
27	Benzophenone	14.4	$C_{13}H_{10}O$	F	+	183.08059	183.08044	0.811	1.83E8	105.03356
28	Spectinomycin	15.33	$C_{14}H_{24}N_2O_7$	C	+	333.16553	333.16563	−0.293	9.54E7	333.16663
29	Diphenylamine	15.41	$C_{12}H_{11}N$	NO	+	170.09640	170.09643	−0.217	3.16E7	170.09625
30	4-Hydroxybenzophenone	15.70	$C_{13}H_{10}O_2$	F# H	+	199.07520	199.07536	−0.784	5.06E6	121.02844, 105.03340
31	(3R)-hydoxy-beta-ionone	15.72	$C_{13}H_{20}O_2$	H	+	209.15385	209.15361	1.165	1.22E7	181.15832, 167.10652, 153.09087, 135.08040
32	4-Methylbenzophenone	16.22	$C_{14}H_{12}O$	F	+	197.09591	197.09609	−0.921	5.58E6	155.08568, 119.04926, 105.03350
33	Decanamide	16.27	$C_{10}H_{21}NO$	C	+	172.16945	172.16959	−0.818	1.05E7	116.10701, 102.09136, 88.07577, 74.06008
34	(1S,3aS,4R,8aS)-1-Hydroxy-4,8a-dimethyloctahydro-6 (1H)-azulenone	16.57	$C_{12}H_{20}O_2$	NO	+	197.15373	197.15361	0.627	1.39E7	141.09088
35	Chalcone	16.59	$C_{15}H_{12}O$	H	+	209.09594	209.09609	−0.725	6.83E6	131.04909, 105.03344, 103.05424
36	Oxybenzone	16.66	$C_{14}H_{12}O_3$	F	+	229.08605	229.08592	0.564	5.60E6	151.03877, 105.03345, 95.04926
37	Bis(2-butoxyethyl) ether	16.91	C12H26O3	F	+	219.19540	219.19547	−0.325	6.09E6	101.09563, 89.05974
38	Methyl + 3,5-di-tert-buty-4-hydroxybenzoate	17.31	$C_{16}H_{24}O_3$	H# F	+	265.18010	265.17982	1.052	5.65E6	209.11678, 163.11090, 153.05420, 149.09636
39	(2S,3S,4S)-4-Amino-2-dodecyltetrahydro-3-furanol	17.71	$C_{16}H_{33}NO_2$	C	+	272.25859	272.25841	0.676	5.79E6	272.25787, 104.07057, 102.05505
40	3,5-Di-tert-butyl-4-hydroxybenzaldehyde	17.83	$C_{15}H_{22}O_2$	F	+	235.16929	235.16926	0.142	9.33E7	235.16896, 179.10649, 123.04409
41	7-Hydroxycoumarine	19.07	$C_9H_6O_3$	F	+	163.03886	163.03897	−0.678	2.50E8	135.04402, 107.04944, 95.04922, 92.02579
42	(-)-D-erythro-Sphingosine	19.85	$C_{18}H_{37}NO_2$	C	+	300.28961	300.28971	−0.319	1.47E7	104.07068
43	Decanophenone	19.63	$C_{16}H_{24}O$	NO	+	233.19003	233.18999	0.163	8.33E6	217.15842, 173.13217, 161.09575
44	Tributyl citrate	20.14	$C_{18}H_{32}O_7$	F	+	361.22211	361.22208	0.084	1.78E8	185.08101,139.00246,129.01817
45	2-Isopropyl-9H-thioxanthen-9-one	20.35	$C_{16}H_{14}OS$	F	+	255.08368	255.08381	−0.519	9.30E6	213.03642
46	Hexadecanamide	22.53	$C_{16}H_{33}NO$	C	+	256.26347	256.26349	−0.083	1.52E7	116.10703, 102.09137, 88.07579
47	Oleamide	22.78	$C_{18}H_{35}NO$	C	+	282.27918	282.27914	0.137	6.80E7	247.24107, 142.12231, 125.09606, 114.09140
48	Stearamide	23.85	$C_{18}H_{37}NO$	C	+	284.29511	284.29479	1.21	1.44E7	130.12250, 116.10699, 102.09135
49	Dioctyl phthalte	24.22	$C_{24}H_{38}O_4$	F	+	391.28455	391.28429	0.674	3.13E7	167.03365, 149.02316
50	Bis(2-ethylhexyl) adipate	24.40	$C_{22}H_{42}O_4$	F	+	371.31531	371.31559	−0.744	1.49E7	143.07007, 129.05453, 111.04407, 101.05969

Abbreviation: Honeysuckle (H); *Fructus forsythia* (F); *Cornu gorais* (C); No known (NO).

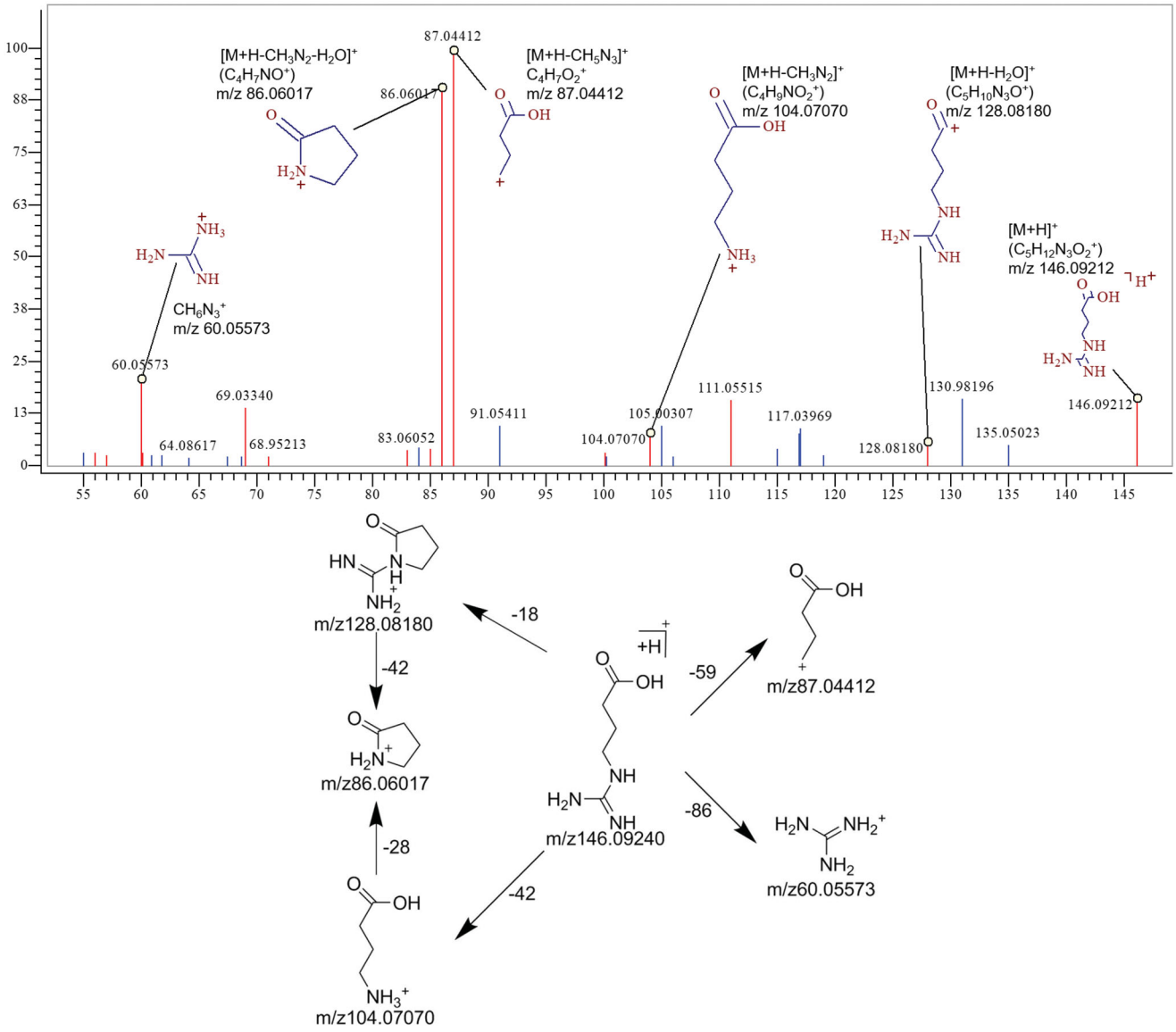

Figure 4. The MS/MS spectrum and the proposed fragmentation pathway of 4-guanidinobutyric acid.

fragment ions $[M+H–H2O]^+$ at *m/z* 88.03944 and $[M+H–HCOOH]^+$at *m/z* 60.04453 were observed, therefore NO. 2 was deduced as D-serine. In the MS/MS analysis of NO. 1 (t_R=0.92 min), the$[M+H–NH_3]^+$ ion at *m/z* 158.09326 was detected, which was cracked from bond C_1–NH_2 and the following splitting decomposition of CO contributed the $[M+H–NH_3–CO]^+$ ion at *m/z* 130.09749. Besides, $[M+H–CN_3H_5]^+$ ion was found at *m/z* 116.07090 which showed that NO. 1 split on the other fragmentation pathway. Therefore, NO. 1 was identified as L-arginine. In addition, many compounds have isomers due to structural diversity, some of which can be distinguished by cracking modes. NO. 10 (t_R=1.00 min) provided $[M+H–HCOOH]^+$ ion at *m/z* 70.06526 as base peak which was formed by the neutral elimination of HCOOH from $[M+H]^+$ ($C_5H_{10}NO_2^+$) ion, and the MS/MS spectra of NO. 10 exhibited product ions $[M+H–H_2O]^+$ ($C_5H_8NO^+$) and $[M+H–CO]^+$ ($C_4H_{10}NO^+$) at *m/z* 98.06017 and *m/z* 88.07590 by the loss of H_2O group and CO. Differently, NO. 4 (t_R=0.96 min) which had the same accurate relative molecular masses and constitutional formula ($C_5H_9NO_2$) with components NO. 10, displayed ion $C_4H_6O_2^+$, $C_4H_8NO^+$, and $C_3H_5N^+$ at *m/z* 85.02845, *m/z* 84.04451, and *m/z* 56.04961 caused by the elimination of neutral groups: CH_2=NH_2, HCHO, and CH_3COOH, respectively. These indicated that NO. 10 was deduced as proline and component NO. 4 and component NO. 10 were mutual isomers, but they were cleaved in different ways. Ultimately, NO. 4 was guessed to be the optical isomer of NO. 10. The proposed fragmentation pathway of NO. 5 were shown in Figure 4. The MS/MS spectra of NO. 5 (t_R =0.96 min) displayed the precursor ion $[M+H]^+$ ($C_5H_{12}N_3O_2^+$) at *m/z* 146.09212 and the fragment ions at *m/z* 128.08180($C_5H_{10}N_3O^+$), 104.07070 ($C_4H_{10}NO_2^+$), 86.06017 ($C_4H_8NO^+$) corresponding to $[M+H–H_2O]^+$, $[M+H–CH_2N_2]^+$, and $[M+H–CH_2N_2–H_2O]^+$. In its MS/MS spectra, the product ions $[M+H–CH_5N_3]^+$ at *m/z* 87.04412 and $CH_6N_3^+$ at *m/z* 60.05573 were observed which suggested the presence of –NHCH(NH_2)=NH unit in the structure. From the above information, NO. 5 was identified

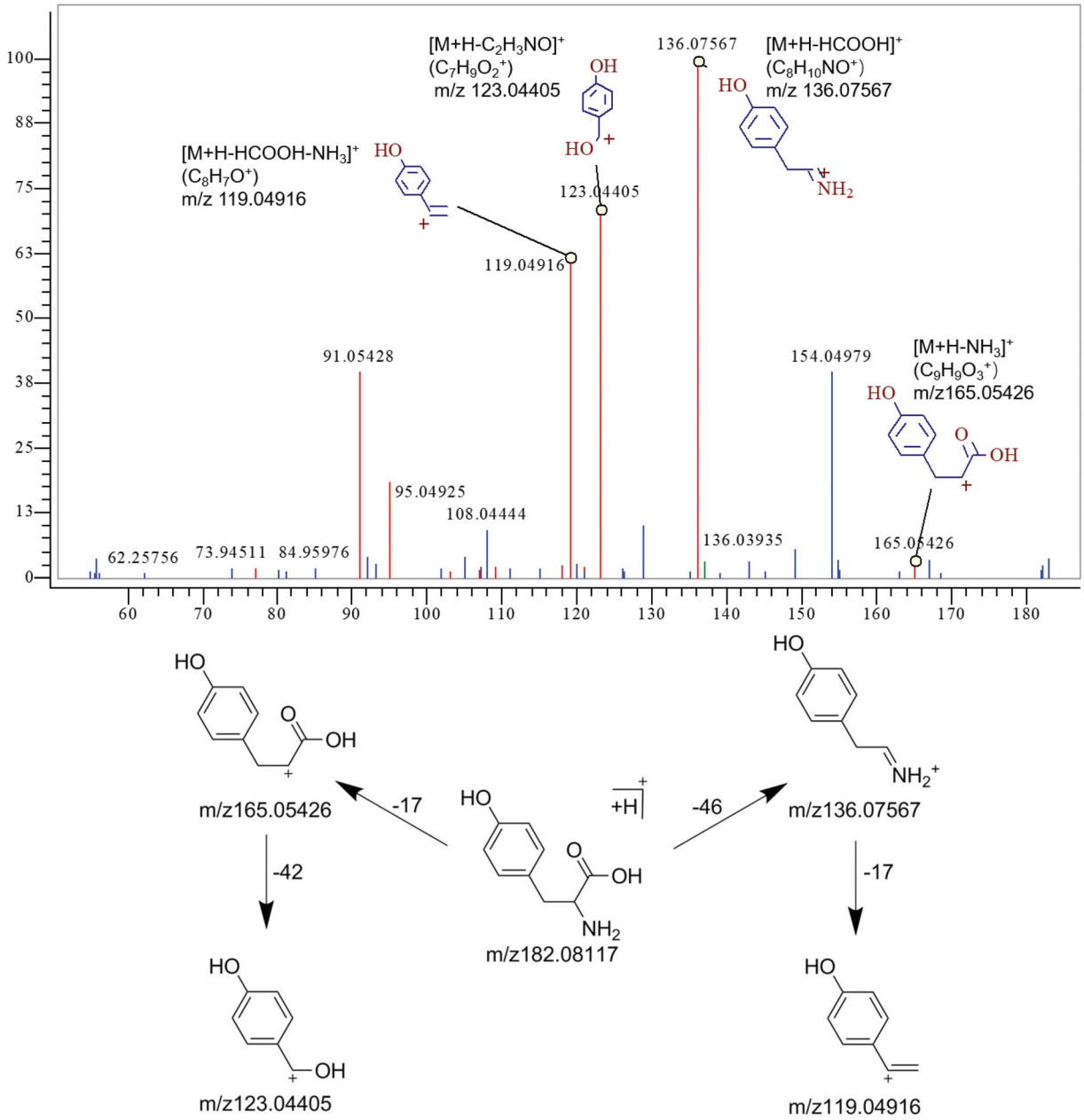

Figure 5. The MS/MS spectrum and the proposed fragmentation pathway of tyrosine.

as 4-guanidinobutyric acid NO. 11 (t_R=1.00 min) gave $[M+H]^+$ ions at *m/z* 120.08079, and obtained fragment ion $[M+H-H_2O]^+$ at *m/z* 102.05499, $[M+H-HCOOH]^+$ at *m/z* 74.06014 and $[M+H-HCOOH-H_2O]^+$ at *m/z* 56.04962. NO. 11 was speculated as Homoserine. As for (NO. 14, t_R=1.02) adenosine which N_9 linked to C_1 of D-Ribose by glycosidic bonds, product ion $[M+H-C_5H_8O_4]^+$ at *m/z* 136.06168 that proved to be the cleavage of glycosidic bonds were showed as base peak in the MS/MS spectra. NO. 16 (t_R=1.39 min) and NO. 18 (t_R=2.38 min) were defined as Tyrosine and L-Phenylalanine, respectively. In the MS/MS experiment of NO. 16 (Figure 5), the major fragments at *m/z* 136.07567 ($C_8H_{10}NO^+$), 123.04405 ($C_7H_9O_2^+$) indicated the loss of HCOOH and C_2H_3NO from the precursor ion, and ion *m/z* 119.04916 ($C_8H_7O^+$) produced by the loss of NH_3 from the *m/z* 136.07567 ion. The other ions in low abundance at *m/z* 165.05426 ($C_9H_9O_3^+$) produced by the loss of NH_3 from the precursor ion. L-Phenylalanine gave base peak ion $[M+H-HCOOH]^+$ at 120.08083.

Long-chain amides are prone to break carbon-carbon single bonds, thereby eliminating long neutral olefin chains. In MS/MS spectra of decanamide (NO. 33, t_R=16.27 min), product ion $[M+H-C_4H_8]^+$ at *m/z* 116.10701, $[M+H-C_5H_{10}]^+$ at *m/z* 102.09136, $[M+H-C_6H_{12}]^+$ at *m/z* 88.07577, and $[M+H-C_7H_{14}]^+$ at *m/z* 74.06008 were discovered. NO. 39 (t_R=17.71 min) obtained the quasi-molecular ion $[M+H]^+$ at *m/z* 272.25787 and fragment ion $[M+H-C_{12}H_{24}]^+$ at *m/z* 104.07057. And the heterocyclic ion containing oxygen pentacyclic ring $[M+H-C_{12}H_{26}]^+$ at *m/z* 102.05505 were yielded in its spectra. $[M+H]^+$ at *m/z* 300.28928, $[M+H-C_{14}H_{28}]^+$ at *m/z* 104.07068 were obtained in the MS/MS spectrum of (-)-D-erythro-sphingosine (NO. 42, t_R=19.58 min). NO. 46 (t_R=22.53 min) and NO. 48 (t_R=23.85 min) exhibited similar fragmentation

pattern. NO. 46 displayed $[M+H]^+$ at *m/z* 256.26306, $[M+H–C_{10}H_{20}]^+$ at *m/z* 116.10703, $[M+H–C_{11}H_{22}]^+$ at *m/z* 102.09137, $[M+H–C_{12}H_{22}]^+$ at *m/z* 88.07579, while NO. 48 gave $[M+H]^+$ at *m/z* 284.29416, $[M+H–C_{11}H_{22}]^+$ at *m/z* 130.12250, $[M+H–C_{12}H_{24}]^+$ at *m/z* 116.10699, $[M+H–C_{13}H_{26}]^+$ at *m/z* 102.09135. NO. 46 and NO. 48 were assigned as hexadecanamide and stearamide, respectively. NO. 47 (t_R=22.85 min) yielded the precursor ion($C_{18}H_{36}NO^+$) $[M+H]^+$ at *m/z* 247.24107 and fragments $C_8H_{16}NO^+$ at *m/z* 142.12231, $C_8H_{13}O^+$ at *m/z* 125.09606, and $C_7H_{16}N^+$ at *m/z*114.09140 indicating the elimination of neutral group Terpene from the precursor ion and the further splitting of NH_3 and CO group. Besides, the product ion $C_{18}H_{33}^+$ at *m/z* 247.24107 was attributed to the loss of NH_2OH from the precursor ion. NO. 48 was surmised as Oleamide, eventually.

According to previous publishes, flavonoids, terpenoids, organic acids and their derivatives and other ingredients are considered as the main chemical constituents of forsythia and these components usually contain carbonyl groups. Theoretically, compounds containing carbonyls are inclined to break of α-C bonds. NO. 6 (t_R=0.96 min) gave $[M+H]^+$ ion ($C_8H_9O_2^+$) at *m/z* 137.05971, and characteristic fragment ions $[M+H–H_2O]^+$ ($C_8H_7O^+$) at *m/z* 119.04897 and $[M+H–HCOOH]^+$ ($C_7H_7^+$) at *m/z* 91.05431 were observed in its MS/MS^2 spectrum. In additional, the prototype ($C_8H_8O_2$) of NO. 6 at *m/z*136.05119 and neutral molecule $[M-C_2H_5O]$ at *m/z* 94.04127 indicated the structure of the component was stable, not easy to crack and the group formyl existed, the unknown component was deduced as 2-acetylphenol. NO. 31 (t_R=15.72 min) showed the $[M+H]^+$ ion as base peak at *m/z* 209.15328 and product ions $[M+H–CO]^+$ at *m/z* 181.15832, $[M+H–C_3H_6]^+$ at *m/z* 167.10652, $[M+H–C_4H_8]^+$ at *m/z* 153.09087, and $C_9H_{11}O^+$ ion at *m/z* 135.08040 which was formed by the further cracking of H_2O loss from $C_9H_{13}O^+$ ion at *m/z* 153.09087. Combining the above information, NO. 31 were speculated as (3R)-hydoxy-beta-ionone by comparing with the retention time and high-resolution accurate mass. NO. 27 (t_R=14.4 min) assigned as Benzophenone displayed $[M+H–C_6H_6]^+$ at *m/z* 105.03356 with extremely high abundance that provided us some basis to presume that groups on both side of carbonyl are benzene rings. Similarly, in the MS/MS spectrum of NO. 30 (t_R=15.70 min) and NO. 32 (t_R=16.22 min), characteristic feature fragments $[M+H–C_6H_6]^+$ at *m/z* 121.02844 and *m/z* 119.04926 were observed, respectively. It demonstrated that NO. 27, NO. 30, and NO. 32 may possess the same skeleton. Also, NO. 30 also obtained the product ion $[M+H-C_6H_6O]^+$ at *m/z* 105.03340 and NO. 32 provided fragment ions $[M+H–C_7H_8]^+$ ($C_7H_5O^+$) at *m/z* 105.03350 and $[M+H–C_2H_2O]^+$ at *m/z* 155.08568, speculating that the chemical structure of NO. 30 and NO. 32 were one more hydroxyl group and one more methyl group than that of NO. 27. So, NO. 30 was inferred to be 4-Hydroxybenzophenone, while NO. 32 was assumed to be 4-Methylbenzophenone. Monoterpenoids often lose neutral groups olefin when they are cracked. In the MS/MS analysis of NO. 13 (t_R=1.01 min), the prototype of the molecular $C_{10}H_{16}O$ at *m/z* 152.07036, the precursor ion $[M+H]^+$ at *m/z* 153.12745, and the product ions $[M+H–CH_4]^+$ ($C_9H_{13}O^+$) at *m/z* 135.08046, $[M+H–C_2H_4]^+$ ($C_8H_{13}O^+$) at *m/z* 125.09651 and $[M+H–C_3H_6]^+$ ($C_7H_{11}O^+$) at *m/z* 111.08058 were detected. And the major fragment ions $C_6H_9O^+$ at *m/z* 97.06476 and $C_8H_{11}^+$ at *m/z* 107.08521 indicated the further splitting of CH_4 and H_2O group from ion $C_8H_{13}O^+$ and $C_9H_{13}O^+$, respectively. Combined with the literatures, NO. 13 may be could identified as pulegone. The MS/MS spectra of aldehydes with longer conjugated chains usually show fragment ions causing by parent ion loss neutral group: H_2O, olefin, and paraffin. For example, NO. 15 (t_R=1.07 min) speculated as 2,4-octadienal yielded quasi-molecular ion $[M+H]^+$ ($C_8H_{13}O^+$), fragment ions $[M+H–CH_4]^+$ ($C_7H_9O^+$) at *m/z* 109.06490, $[M+H–H_2O]^+$ ($C_8H_{11}^+$) at *m/z* 107.08566, $[M+H–C_2H_6]^+$ ($C_6H_7O^+$) at *m/z* 95.04921, $[M+H–C_3H_6]^+$ ($C_5H_7O^+$) at *m/z* 83.04933, $[M+H–C_3H_8]^+$ ($C_5H_5O^+$) at *m/z* 81.07001. In the MS/MS spectrum of NO. 40 (t_R=17.83 min), the product ions $C_{11}H_{15}O_2^+$ at *m/z* 179.10649 and $C_7H_7O_2^+$ at *m/z* 123.04409 attributed to the successively two C_4H_8 units removement from ion $[M+H]^+$ ($C_{15}H_{23}O_2^+$) were monitored and proved the existence of two tert-butyl groups in its chemical structure. Then, NO. 40 was inferred to be 3,5-di-tert-butyl-4-hydroxybenzaldehyde.

In term of phenolic acids containing phenolic hydroxyl groups and carboxyl groups, their MS/MS spectrums show the elimination of neutral molecules such as H_2O, HCOOH, HCHO, and CO. NO. 25 was referred to be phenolic acid derivative: diethyl phthalate. In the MS/MS experiment of NO. 25, the ion $[M+H–2C_2H_4]^+$ ($C_8H_7O_4^+$) at *m/z* 167.03365 was observed as base peak ion, and the ion $[M+H–2C_2H_4–H_2O]^+$ at *m/z* 149.02316 was detected. Those ions demonstrated the presence of two ethyl groups, the breakdown of ester bonds, and the dehydration and condensation of two adjacent carboxyl groups on the benzene ring. So, NO. 25 was tentatively identified as diethyl phthalate. Since most flavonoids contain multiple hydroxyl groups, $[M+H–H_2O]^+$ ions are always the characteristic ion of most flavonoids. However, the pyrolysis manners of flavonoids are various due to quite disparity in their structural formulas. For instance, NO. 23 (t_R=7.82 min) which deduced as genistein ($C_{15}H_{10}O_5$) gave $[M+H]^+$ as base peak ion at *m/z* 271.05972 and fragment ion $[M+H–H_2O]+$ ions ($C_{15}H_9O_5^+$) at *m/z* 253.04889. Similarity, NO. 26 (t_R=13.75 min) speculated as glycitein also displayed $[M+H]^+$ ($C_{16}H_{13}O_5^+$) as base peak ion, and showed ion $[M+H–H_2O]^+$ ($C_{16}H_{11}O_4^+$) at *m/z* 253.05019 and neutral molecular $C_{15}H_9O_5$ at *m/z* 270.05188. In the MS/MS spectrum of NO. 35 (t_R=16.59 min), the elimination of C_6H_6 from precursor ion contributed to the $[M+H–C_6H_6]^+$ ($C_9H_4O^+$) at *m/z* 131.04909. The other product ions $[M+H–H_8O_8]^+$ ($C_7H_5O^+$) and $[M+H–C_7H_6O]^+$ ($C_8H_7^+$) resulted from two pattern of fracturing the same bond. Combined with retention time, accurate mass and literature, NO. 35 was ultimately deduced as chalcone. NO. 37 (t_R= 16.91 min) and NO. 50

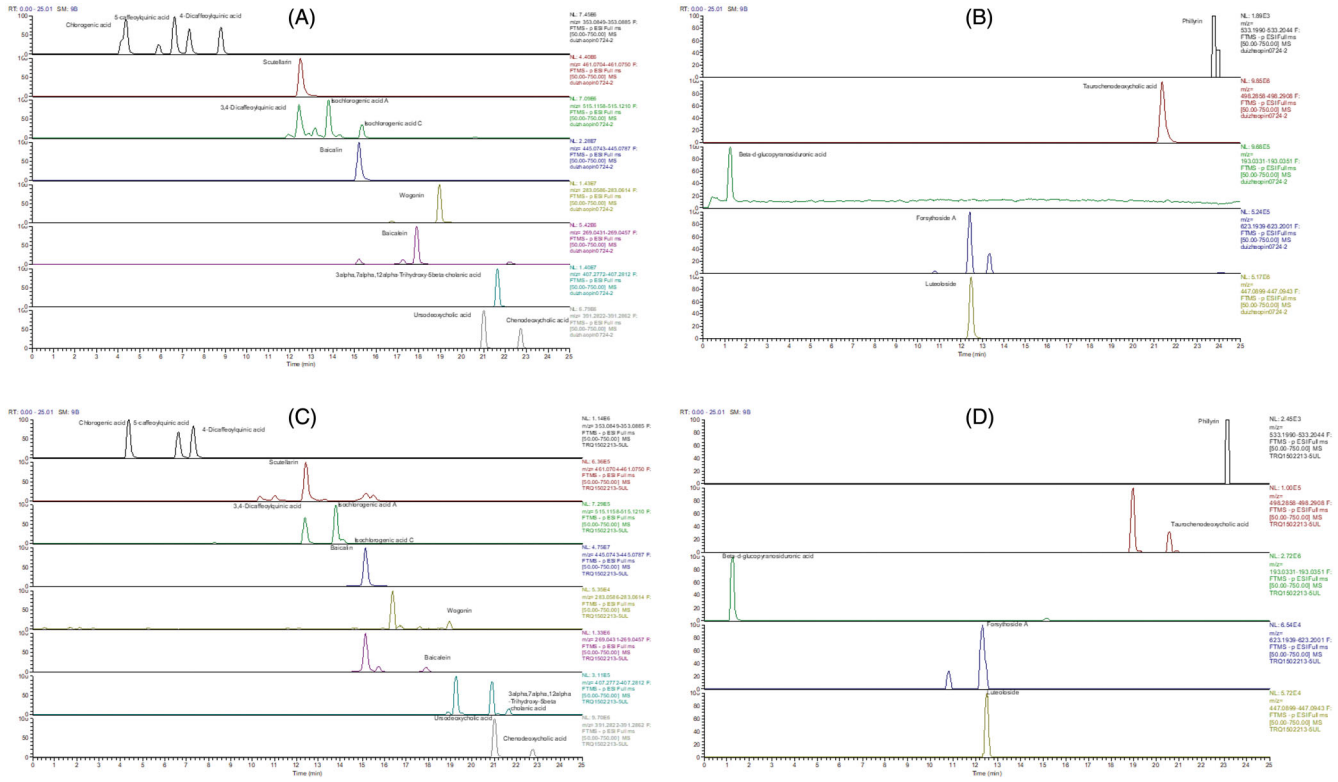

Figure 6. The full scan mass spectra of reference standards (A, B) and Tanreqing injection samples.

(t_R=24.40 min) possessed the similar fracture manner. According to the ions: $[M+H–C_6H_{14}O_2]^+$ ($C_6H_{13}O^+$) at *m/z* 101.09563 and $[M+H–C_8H_{18}O]^+$ ($C_4H_9O_2^+$) at *m/z* 89.05974 observed in the MS/MS of spectrum of NO. 37 and the ion: $[M+H–C_{15}H_{32}O]^+$ ($C_7H_{11}O_3^+$) at *m/z* 143.07007, $[M+H–C_{16}H_{34}O]^+$ ($C_6H_9O_3^+$) at *m/z* 129.05453, $[M+H–C_{16}H_{34}O–H_2O]^+$ ($C_6H_7O_2^+$) at *m/z* 111.04407 and $[M+H–C_{16}H_{34}O–CO]^+$ ($C_5H_9O_2^+$) at *m/z* 101.05969 the NO. 50 (t_R=24.40 min) showed, NO. 37 and NO. 50 were assigned as bis(2-butoxyethyl) ether and bis(2-ethylhexyl) adipate, respectively.

Quantitative analysis of samples

Method validation

In order to verify the rationality of the optimized method, we conducted methodology validation of selectivity, linearity, limit of detection (LOD), limit of quantification (LOQ), precision, repeatability, recovery, and stability.

Selectivity. The full scan mass spectra of the above mentioned 18 components in TRQI under the optimal condition that described in Section "Chromatographic and mass spectrometric condition " were shown in Figure 6. According to the full scan mass spectra, we conclude that no interference was found between the peaks and peak shape was good.

Linearity, LOD, and LOQ. A mixed standard solution containing 18 compound controls was prepared and then diluted into 6 concentration gradient series to obtain calibration curves. When calculating the linear regression equation, the concentration value of the measured components was set as the X-axis, and the peak area value of the measured components was set as the Y-axis. The LOD and LOQ under optimized chromatographic conditions were determined at S/N = 3 and 10, respectively. The regression equation, correlation coefficient (*r*), linear range, LOD, and LOQ of the 18 components that were quantitatively analyzed are shown in Table S1 (Supplementary material). The results demonstrated that all the 18 analytes showed a good linear relationship with r values greater higher than 0.995, and the LOD (0.045–0.763 ng/mL) and LOQ (0.147–2.607 ng/mL) values are within the range that satisfy the required requirements.

Precision, stability, and repeatability. To evaluate the precision of the instrument, intra-day variability was tested with the mixture standard solutions during a day, inter-day variability was measured during three consecutive days. At room temperature, the stability of the sample solutions and the standard control solutions for three consecutive days at 0 h, 12 h, 24 h, 36 h, 48 h, 60 h, and 72 h were analyzed. The prepared 6 sets of TRQI sample solutions were analyzed in parallel to examine the repeatability of the samples. Of course, the 6 sets of TRQI sample solutions were prepared from the same batch of TRQI. The precision, Stability and Repeatability results of 18 compounds were expressed as relative standard deviation (RSD) and shown in Table S2 (Supporting material). Regarding the precision results, the RSD values of majority of compounds were below 3.00%, which was a satisfactory result and the intra-day RSD values of 4-Dicaffeoylquinic acid and 3,4-Dicaffeoylquinic acid are 3.15 and 4.01%, respectively, which are within the acceptable

scope. As for stability, the RSD values of the 18 analytes were all below 3.07%, indicating that all analytes in the sample solution and the reference standard solution were sufficiently stable. Repeatability results of 18 compounds depicted that RSD values were less than 3.00%. Comprehensive analysis presented that the experimental method adhered good precision, stability, and repeatability.

Recovery. Recovery was verified by adding different concentrations (high, medium, low, $n = 3$) at 80%, 100%, and 120% known amounts of stock standard into one samples of known concentration, respectively. Each level was performed in triplicate and the results were calculated by the following formula: recovery (%) = (amount detected – original amount)/amount spiked × 100. The recovery results of 18 components were displayed in Table S2 (Supporting material), and the RSD was employed as a measured index. The recovery of the 18 compounds were in the range of 97.25–102.42% with the RSD values were less than 2.27%, which showed the recovery of samples were satisfied.

Quantitative results of TRQI

According to the principle of Theoretical Basis of Traditional Chinese Medicine, the five herbs in TRQI served as different roles, *Scutellaria* the root of eliminating heat and eliminating toxin was monarch drug in TRQI, Goat horn, and bear gallbladder powder which enhanced the effect of *Scutellaria* were used as ministers' medicine and *Honeysuckle* was regarded as adjuvant. Therefore, baicalin, the main component in bear bile powder, chlorogenic acid and its derivatives in honeysuckle, forsythoside A and phillyrin in *Fructus forsythiae* were detected as index components. Amino acids in *Cornu gorais* are mostly endogenous components, so amino acids were not elected as quantitative indexes, On the contrary, scutellarin and baicalein the commonly derivative of baicalin were optimized as markers. The 18 components of TRQI in three batches were quantitatively analyzed by utilizing UHPLC-Q-Orbitrap method. Analyze each corresponding component according to the corresponding calibration curve determining and determine the quantitative results by three parallel experiments. Table 4 and Figure 7 presented the quantitative results of the 18 representative components in the 8 batches of TRQI. The results showed that the content of the 18 components was quite different. Beta-d-glucopyranosiduronic acid, baicalin, ursodeoxycholic acid, and chenodeoxycholic acid were the predominant constituents, 4-dicaffeoylquinic acid, scutellarin, and isochlorogenic acid C presented moderate contents levels. Baicalin showed highest amounts in 8 batches, ursodeoxycholic acid followed by, both of wogonin and taurochenodeoxycholic acid displayed the lowest amount. In the same sample, the highest content of ingredients is almost 60,000 times higher than the lowest content of ingredients. High and low constituents can be quantified in one analysis proving the higher resolution and superior selectivity of the validated method. Comparing the contents of each component in different batches, it was found that the distinction between the high-content components was not significant,

Table 4. The quantitative results of the 18 components in three batches of TRQI/(μg mL^{-1}).

	Batch							
Analyte	1809203	1806211	1806208	1807209	1805210	1809206	1807215	1812208
Beta-d-glucopyranosiduronic acid	3329.01 ± 79.62	4255.02 ± 106.32	3529.46 ± 94.05	3829.61 ± 72.59	3697.15 ± 62.00	4077.07 ± 54.06	2951.97 ± 45.82	3946.71 ± 66.16
Chlorogenic acid	320.99 ± 9.99	346.10 ± 3.52	285.73 ± 7.12	248.67 ± 4.09	310.29 ± 5.58	293.84 ± 6.00	278.71 ± 3.99	268.3 ± 7.08
5-Caffeoylquinic acid	59.63 ± 1.65	42.97 ± 0.74	68.24 ± 1.33	47.99 ± 0.86	57.49 ± 0.49	53.79 ± 0.71	71.35 ± 0.22	64.16 ± 1.20
4-Dicaffeoylquinic acid	142.01 ± 5.72	91.25 ± 1.09	176.97 ± 6.28	127.53 ± 6.97	156.44 ± 2.34	135.76 ± 4.50	187.66 ± 1.76	136.27 ± 3.19
Forsythoside A	7.95 ± 0.17	4.97 ± 0.14	6.47 ± 0.13	8.02 ± 0.09	7.28 ± 0.07	5.2 ± 0.05	7.41 ± 0.01	6.81 ± 0.11
3,4-Dicaffeoylquinic acid	33.88 ± 2.40	12.66 ± 1.13	27.92 ± 1.76	39.62 ± 0.62	28.51 ± 1.10	23.68 ± 1.32	30.16 ± 0.89	37.92 ± 1.22
Scutellarin	85.49 ± 6.15	82.61 ± 7.48	87.63 ± 5.98	89.02 ± 2.60	83.02 ± 3.14	90.11 ± 4.91	86.19 ± 1.74	81.04 ± 6.15
Luteoloside	5.42 ± 0.19	4.18 ± 0.04	2.95 ± 0.15	2.57 ± 0.11	4.12 ± 0.09	3.95 ± 0.18	6.07 ± 0.14	5.41 ± 0.16
Isochlorogenic acid A	75.13 ± 0.77	48.17 ± 0.28	57.94 ± 0.49	81.01 ± 0.47	63.4 ± 0.45	54.67 ± 0.36	56.18 ± 0.56	69.14 ± 0.55
Isochlorogenic acid C	412.66 ± 10.33	373.66 ± 12.03	468.55 ± 9.81	434.00 ± 8.29	436.18 ± 4.06	395.33 ± 4.72	477.31 ± 2.74	435.77 ± 6.42
Baicalin	5864.48 ± 82.14	5806.44 ± 76.33	5940.54 ± 73.44	5951.02 ± 82.09	5934.15 ± 27.13	5862.13 ± 69.43	6032.17 ± 108.52	5976.16 ± 84.06
Baicalein	6.34 ± 0.07	8.73 ± 0.19	6.84 ± 0.15	4.23 ± 0.04	5.91 ± 0.10	4.95 ± 0.08	3.61 ± 0.24	5.81 ± 0.14
Phillyrin	10.81 ± 1.97	3.89 ± 0.07	8.46 ± 0.74	9.10 ± 0.10	10.65 ± 0.10	9.54 ± 0.37	13.00 ± 0.06	10.46 ± 0.57
Wogonin	0.54 ± 0.01	0.18 ± 0.01	0.48 ± 0	0.81 ± 0	0.64 ± 0.01	0.34 ± 0	0. 19 ± 0	0.46 ± 0.01
Taurochenodeoxycholic acid	2.48 ± 0.01	2.79 ± 0.03	2.64 ± 0.03	2.45 ± 0.02	2.48 ± 0.03	2.44 ± 0.01	1.99 ± 0.04	2.96 ± 0.04
3α,7α,12α-Trihydroxy-5beta-cholanic acid	11.64 ± 0.09	19.04 ± 0.02	9.54 ± 0.08	4.71 ± 0.09	10.64 ± 0.04	7.94 ± 0.04	3.11 ± 0.01	8.94 ± 0.10
Ursodeoxycholic acid	5493.14 ± 17.94	5007.63 ± 14.15	5498.46 ± 22.11	5521.11 ± 34.01	5416.42 ± 19.55	4998.18 ± 14.70	5155.10 ± 18.38	5349.49 ± 25.94
Chenodeoxycholic acid	1794.46 ± 32.88	1567.19 ± 29.41	1585.26 ± 27.11	1599.73 ± 24.70	1674.58 ± 23.09	1577.56 ± 27.49	1943.28 ± 33.98	1843.22 ± 31.07

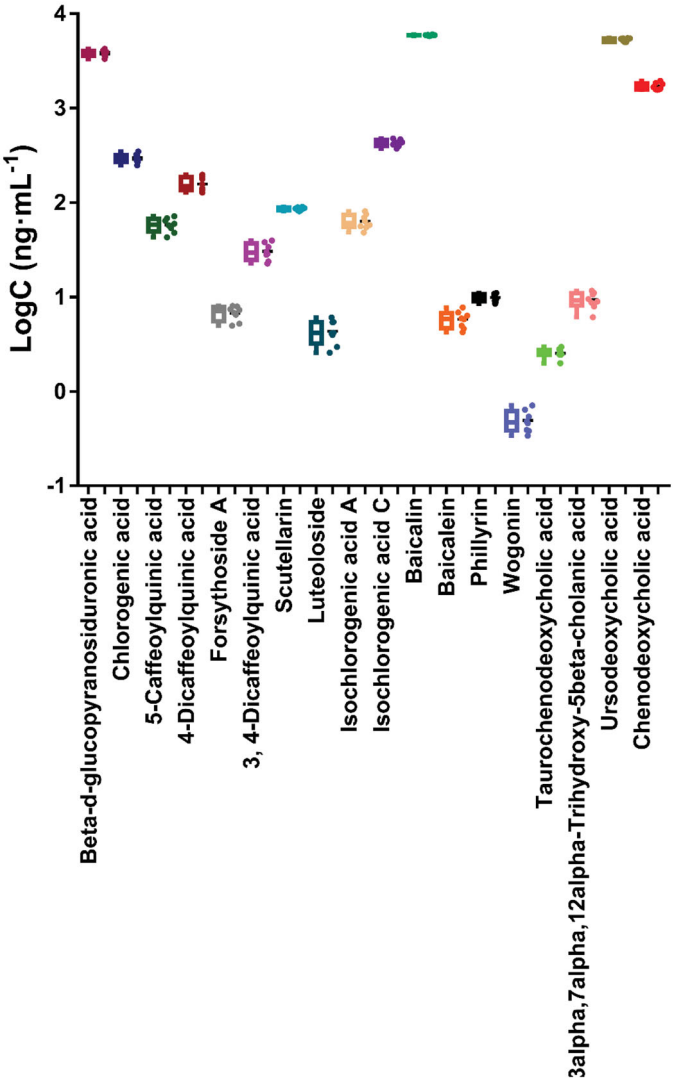

Figure 7. Quantitative results of the 18 representative components in the 8 batches of TRQI.

while the greater disparity was between the low-content components. For example, the amount of Wogonin in batch 18,06,211 was approximately 3.5 times higher than that in batch 18,07,209. From another perspective, the major components: baicalin, beta-d-glucopyranosiduronic acid, ursodeoxycholic acid, and chenodeoxycholic acid were derived from *Scutellaria baicalensis*, *Honeysuckle* and *Bear gallbladders powder*, respectively. The results were consistent with the theory of compatibility of Chinese medicine compound prescription. Thus, combining the quantitative analysis results with the compatibility principle of traditional Chinese medicine, it was speculated that beta-d-glucopyranosiduronic acid, chlorogenic acid, 4-dicaffeoylquinic acid, scutellarin, isochlorogenic acid C, baicalin, ursodeoxycholic acid, and chenodeoxycholic acid may be the primary effectors, while 5-caffeoylquinic acid, 3,4-dicaffeoylquinic acid and isochlorogenic acid A may be used primarily to enhance the potency of major constituents. In addition, Principal components analysis was performed according the quantitative determinations in 8 batches of Tanreqing injection. As a result, five principal components were extracted, and the variance contribution rates of the five principal components were ranked as: 37.86, 22.86, 16.42, 9.80, 7.32%, with the accumulated value 94.26%. Considering the Figure 8 which displayed the factor loading results of these 18 components in factor 1, factor 2 and factor 3, variable 5-caffeoylquinic acid, isochlorogenic acid C, and baicalin possessed larger loads on the first factor, variable 3,4-dicaffeoylquinic acid and isochlorogenic acid A harbored greater loads on the second factor, and variable forsythoside A, wogonin and ursodeoxycholic acid occupied the dominant loads on the third factor. Therefore, it is speculated that 5-caffeoylquinic acid, isochlorogenic acid C, isochlorogenic acid A, 3,4-dicaffeoylquinic acid, baicalin, forsythoside A, wogonin and ursodeoxycholic acid may be the main reason for the quality difference between different batches. This study provides a

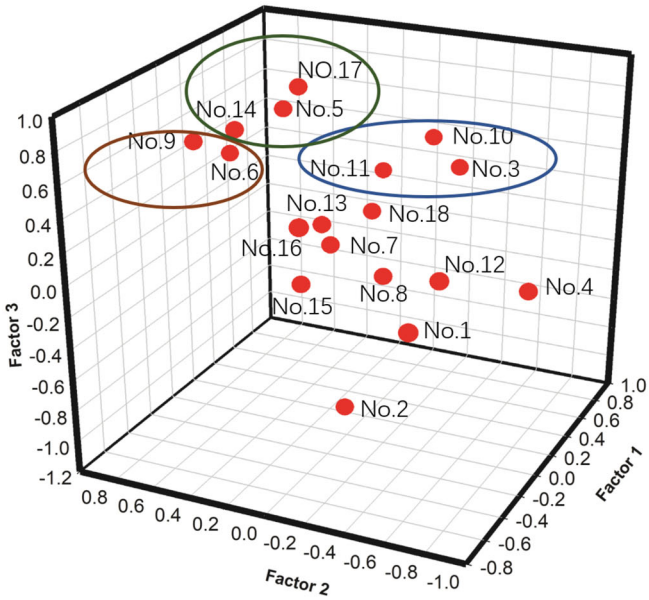

No.1 (Beta-d-glucopyranosiduronic acid)
No.2 (Chlorogenic acid)
No.3 (5-Caffeoylquinic acid)
No.4 (4-Dicaffeoylquinic acid)
No.5 (Forsythoside A)
No.6 (3,4-Dicaffeoylquinic acid)
No.7 (Scutellarin)
No.8 (Luteoloside)
No.9 (Isochlorogenic acid A)
No.10 (Isochlorogenic acid C)
NO.11 (Baicalin)
NO.12 (Baicalein)
NO.13 (Phillyrin)
NO.14 (Wogonin)
NO.15 (Taurochenodeoxycholic acid)
NO.16 (3alpha,7alpha,12alpha-Trihydroxy-5beta-cholanic acid)
NO.17 (Ursodeoxycholic acid)
NO.18 (Chenodeoxycholic acid)

Figure 8. The factor loads of the 18 components in Factor 1, Factor 2, and Factor 3.

certain experimental reference for the selection of quality markers for Tanreqing Injection.

Conclusion

In this paper, the chemical constituents of TRQI was qualitatively identified with the utilization of UPLC-Q-Orbitrap mass spectrometry and the contents of 18 characteristic components in three batches TRQI were measured. According to the accurate mass of the constituents and the cleavage pathway, 80 unknown components such as flavonoids, amino acids, coumarins, and cholic acids were deduced, and 18 of them were confirmed unambiguously by the comparison with corresponding reference. On the basis of qualitative research, the contents of 18 representative components was determined in 8 batches of TRQI samples. In the study, the experimental method showed high sensitivity, strong specificity, good stability, and reasonable recovery rate, which proved the applicability of the method. Therefore, UHPLC-Q-Orbitrap mass spectrometry method shown sensitivity, accuracy, and time-saving advantages in the basic researches on compounded Chinese medicinal prescription, and can be applied for simultaneously quantitative detection of multiple components. This study not only enriched the research on the chemical constituents in Tanreqing injection, provided a theoretical basis for pharmacodynamics basic research about traditional Chinese medicine compound, but also provided a certain experimental reference for the selection of quality markers of Tanreqing injection, which was far-reaching significance for the quality control of traditional Chinese medicine compounds.

Acknowledgments

The authors thanks all the volunteers involved in the study and all the people in the Co-construction Collaborative Innovation Center for Chinese Medicine and Respiratory Diseases by Henan & Education Ministry of P.R. for their help. Both of these laboratories contributed to the study design, research, interpretation of data, and the writing, reviewing, approving of the publication. The authors declare no conflict of interest.

Funding

This research was supported financially by Co-construction Collaborative Innovation Center for Chinese Medicine and Respiratory Diseases by Henan & Education Ministry of P. R. and Zhengzhou Key Laboratory of Chinese Medicine Quality Control and Evaluation (project number: 20A360007, BSJJ-2016-01).

References

[1] Yu, J.; Li, Y.; Liu, X.; Ma, Z.; Michael, S.; Orgah, J. O.; Fan, G.; Zhu, Y. Mitochondrial Dynamics Modulation as a Critical Contribution for Shenmai Injection in Attenuating Hypoxia/Reoxygenation Injury. *J. Ethnopharmacol.* **2019**, *237*, 9–19. DOI: 10.1016/j.jep.2019.03.033.

[2] Duan, Z. Z.; Li, Y. H.; Li, Y. Y.; Fan, G. W.; Chang, Y. X.; Yu, B.; Gao, X. M. Danhong Injection Protects Cardiomyocytes against Hypoxia/Reoxygenation- and H_2O_2-Induced Injury by Inhibiting Mitochondrial Permeability Transition Pore Opening. *J. Ethnopharmacol.* **2015**, *175*, 617–625. DOI: 10.1016/j.jep.2015.08.033.

[3] Gu, Y. Y.; Shi, L.; Zhang, D. D.; Huang, X.; Chen, D. Z. Metabonomics Delineates Allergic Reactions Induced by Shuang-Huang-Lian Injection in Rats Using Ultra Performance Liquid Chromatography-Mass Spectrometry. *Chin. J. Nat. Med.* **2018**, *16*, 628–640. DOI: 10.1016/S1875-5364(18)30101-8.

[4] Li, H. N.; Wang, S. W.; Yue, Z. H.; Ren, X. Q.; Xia, J. L. Traditional Chinese Herbal Injection: Current Status and Future Perspectives. *Fitoterapia.* **2018**, *129*, 249–256. DOI: 10.1016/j.fitote.2018.07.009.

[5] Wang, L.; Cheng, L.; Yuan, Q.; Cui, X. H.; Shang, H. C.; Zhang, H. C.; Zhang, B. L.; Li, Y. P. Adverse Drug Reactions of Shuanghuanglian Injection: A Systematic Review of Public Literatures. *J. Evid. Based Med.* **2010**, *3*, 18–26. DOI: 10.1111/j.1756-5391.2010.01067.x.

[6] Wang, L.; Cui, X.; Cheng, L.; Yuan, Q.; Li, T.; Li, Y.; Deng, S.; Shang, H.; Bian, Z. Adverse Events to Houttuynia Injection: A Systematic Review. *J. Evid. Based Med.* **2010**, *3*, 168–176. DOI: 10.1111/j.1756-5391.2010.01091.x.

[7] Sun, Z.; Zuo, L.; Sun, T.; Tang, J.; Ding, D.; Zhou, L.; Kang, J.; Zhang, X. Chemical Profiling and Quantification of XueBiJing Injection, a Systematic Quality Control Strategy Using UHPLC-Q Exactive Hybrid Quadrupole-Orbitrap High-Resolution Mass Spectrometry. *Sci. Rep.* **2017**, *7*, 16921. DOI: 10.1038/s41598-017-17170-y.

[8] Yang, Y.; Wang, H. J.; Brantner, A. H.; Lower-Nedza, A. D.; Si, N.; Song, J. F.; Bai, B.; Zhao, H. Y.; Bian, B. L. Chemical Profiling and Quantification of Chinese Medicinal Formula Huang-Lian-Jie-Du Decoction, a Systematic Quality Control Strategy Using Ultra High Performance Liquid Chromatography Combined with Hybrid Quadrupole-Orbitrap and Triple Quadrupole Mass Spectrometers. *J. Chromatogr.* **2013**, *1321*, 88–99. DOI: 10.1016/j.chroma.2013.10.072.

[9] Zhang, Y. W.; Cheng, Y. C. Challenge and Prospect of Traditional Chinese Medicine in Depression Treatment. *Front. Neurosci.* **2019**, *13*, 190. DOI: 10.3389/fnins.2019.00190.

[10] Zhao, J.; Ma, S. C.; Li, S. P. Advanced Strategies for Quality Control of Chinese Medicines. *J. Pharm. Biomed. Anal.* **2018**, *147*, 473–478. DOI: 10.1016/j.jpba.2017.06.048.

[11] Wang, P.; Liao, X.; Xie, Y. M.; Chai, Y.; Li, L. H. Tanreqing Injection for Acute Bronchitis Disease: A Systematic Review and Meta-Analysis of Randomized Controlled Trials. *Complement Ther. Med.* **2016**, *25*, 143–158. DOI: 10.1016/j.ctim.2016.02.008.

[12] Xiong, L.; Chen, L.; Wang, C. Q.; Yue, J. B.; Li, Y. Q.; Zhou, W. J.; Yuan, Y.; Liu, Q. X.; Xiao, Z. Clinical Efficacy and Safety of Tanreqing Injection for Pulmonary Infection in Patients with Tuberculosis: A Meta-Analysis. *J. Altern. Complement Med.* **2018**, *24*, 1051–1062. DOI: 10.1089/acm.2018.0020.

[13] Fan, Y.; Yang, T.; Zheng, Q.; Wang, L.; Yuan, C.; Fang, L.; Li, K. Protective Effect of Tanreqing Injection on Axon Myelin Damage in the Brain of Mouse Model for Experimental Autoimmune Encephalomyelitis. *J. Tradit. Chin. Med.* **2014**, *34*, 576–583. DOI: 10.1016/S0254-6272(15)30066-2.

[14] Li, X. X.; Zhou, L.; Yang, Y. H.; Zhan, S. Y.; Zhai, S. D. Post-Marketing Surveillance of Tanreqing Injection in Children: A Real World Study. *Chin. J. Epidemiol.* **2017**, *38*, 248–252.

[15] Li, Y. Y.; Qi, L. K.; Lin, L. Z.; Kong, J. Y. Simultaneous Determination of Seven Flavonoids in Dalbergiae Odoriferae Lignum by UPLC and Principal Component Analysis. *Chin. J. Pharm. Anal.* **2019**, *39*, 240–248.

[16] Zhang, F.; Sun, L.; Gao, S. H.; Chen, W. S.; Chai, Y. F. LC-MS/MS Analysis and Pharmacokinetic Study on Five Bioactive Constituents of Tanreqing Injection in Rats. *Chin. J. Nat. Med.* **2016**, *14*, 769–775. DOI: 10.1016/S1875-5364(16)30091-7.

[17] Zhao, Y. N.; Xu, Z. Y.; Wang, T. M.; Li, Y. Y.; Yang, L.; Liu, S. Y.; Shi, R.; Ma, Y. M. Simultaneous Quantitation of 23 Bioactive Compounds in Tanreqing Capsule by

High-Performance Liquid Chromatography Electrospray Ionization Tandem Mass Spectrometry. *Biomed. Chromatogr.* **2019**, *33*, e4531. DOI: 10.1002/bmc.4531.

[18] Li, C.; Zang, C.; Nie, Q. X.; Yang, B.; Zhang, B. X.; Duan, S. F. Simultaneous Determination of Seven Flavonoids, Two Phenolic Acids and Two Cholesterines in Tanreqing Injection by UHPLC-MS/MS. *J. Pharm. Biomedical. Anal.* **2019**, *30*, 105–112. DOI: 10.1016/j.jpba.2018.08.058.

[19] Liu, S. Y.; Xue, D. S.; Pan, J. C.; Zhang, W. M.; Li, W. L.; Qu, H. B. Screening and Identification of Multiple Components in Tanreqing Injection Using RP-HPLC Combined with DAD and ESI-TOF/MS. *Chin. J. Nat. Med.* **2014**, *12*, 535–541. DOI: 10.1016/S1875-5364(14)60083-2.

[20] Sun, L.; Wei, H.; Zhang, F.; Ga, S. H.; Zeng, Q. H.; Lu, W. Q.; Chen, W. S.; Chai, Y. F. Qualitative Analysis and Quality Control of Traditional Chinese Medicine Preparation Tanreqing Injection by LC-TOF/MS and HPLC-DAD-ELSD. *Anal. Methods*. **2013**, *5*, 6431–6440. DOI: 10.1039/c3ay40681d.

[21] Dong, J.; Zhu, Y.; Gao, X.; Chang, Y.; Wang, M.; Zhang, P. Qualitative and Quantitative Analysis of the Major Constituents in Chinese Medicinal Preparation Dan-Lou Tablet by Ultrahigh Performance Liquid Chromatography/Diode-Array Detector/Quadrupole Time-of-Flight Tandem Mass Spectrometry. *J. Pharm. Biomed. Anal.* **2013**, *80*, 50–62. DOI: 10.1016/j.jpba.2013.02.011.

[22] Lv, X. J.; Sun, Z.; Wang, P. L.; Yang, J.; Xu, T. Y.; Jia, Q. Q.; Li, D. W.; Su, F. Y.; Zhu, Z. F.; Kang, J.; Zhang, X. J. Chemical Profiling and Quantification of Dan-Deng-Tong-Nao-Capsule Using Ultra High Performance Liquid Chromatography Coupled with High Resolution Hybrid Quadruple-Orbitrap Mass Spectrometry. *J. Pharm. Biomed. Anal.* **2018**, *148*, 189–204. DOI: 10.1016/j.jpba.2017.09.034.

[23] Yan, B.; Xu, W.; Su, S.; Zhu, S.; Zhu, Z.; Zeng, H.; Zhao, M.; Qian, D.; Duan, J. A. Comparative Analysis of 15 Chemical Constituents in *Scutellaria Baicalensis* Stem-Leaf from Different Regions in China by Ultra-High Performance Liquid Chromatography with Triple Quadrupole Tandem Mass Spectrometry. *J. Sep. Sci.* **2017**, *40*, 3570–3581. DOI: 10.1002/jssc.201700473.

[24] Qiao, X.; Li, R.; Song, W.; Miao, W. J.; Liu, J.; Chen, H. B.; Guo, D. A.; Ye, M. A Targeted Strategy to Analyze Untargeted Mass Spectral Data: Rapid Chemical Profiling of *Scutellaria Baicalensis* Using Ultra-High Performance Liquid Chromatography Coupled with Hybrid Quadrupole Orbitrap Mass Spectrometry and Key Ion Filtering. *J. Chromatogr. A.* **2016**, *1441*, 83–95. DOI: 10.1016/j.chroma.2016.02.079.

[25] Liu, G.; Rajesh, N.; Wang, X.; Zhang, M.; Wu, Q.; Li, S.; Chen, B.; Yao, S. Identification of Flavonoids in the Stems and Leaves of *Scutellaria Baicalensis* Georgi. *J. Chromatogr. B Analyt. Technol. Biomed. Life Sci.* **2011**, *879*, 1023–1028. DOI: 10.1016/j.jchromb.2011.02.050.

[26] Dong, Z. L.; Lu, X. Y.; Tong, X. L.; Dong, Y. Q.; Tang, L.; Liu, M. H. Forsythiae Fructus: A Review on Its Phytochemistry, Quality Control, Pharmacology and Pharmacokinetics. *Molecules.* **2017**, *22*, pii:1466. DOI: 10.3390/molecules22091466.

[27] Du, K. Z.; Li, J.; Li, J.; Tian, F.; Chang, Y. X. Non-Ionic Detergent Triton X-114 Based Vortex- Synchronized Matrix Solid-Phase Dispersion Method for the Simultaneous Determination of Six Compounds with Various Polarities from Forsythiae Fructus by Ultra High-Performance Liquid Chromatography. *J. Pharm. Biomed. Anal.* **2018**, *150*, 59–66. DOI: 10.1016/j.jpba.2017.12.003.

[28] Zhang, B.; Nan, T. G.; Xin, J.; Zhan, Z. L.; Kang, L. P.; Yuan, Y.; Wang, B. M.; Huang, L. Q. Development of a Colloidal Gold-Based Lateral Flow Dipstick Immunoassay for Rapid Detection of Chlorogenic Acid and Luteoloside in Flos Lonicerae Japonicae. *J. Pharm. Biomed. Anal.* **2019**, *170*, 83–88. DOI: 10.1016/j.jpba.2019.03.035.

[29] Mei, Y. D.; Pan, D. B.; Jiang, Y. N.; Zhang, W. Y.; Yao, X. J.; Dai, Y.; Yu, Y.; Yao, X. S. Target Discovery of Chlorogenic Acid Derivatives from the Flower Buds of Lonicera Macranthoides and Their MAO B Inhibitory Mechanism. *Fitoterapia.* **2019**, *134*, 297–304. DOI: 10.1016/j.fitote.2018.12.009.

[30] Bi, D.; Chai, X. Y.; Song, Y. L.; Lei, Y.; Tu, P. F. Novel Bile Acids from Bear Bile Powder and Bile of Geese. *Chem. Pharm. Bull.* **2009**, *57*, 528–531. DOI: 10.1248/cpb.57.528.

[31] Jian, L. H.; Mao, X. H.; Wang, K.; Ji, S. Structure Determination of Three Novel Bile Acids from Bear Bile Powder. *Yao. Xue. Xue. Bao.* **2013**, *48*, 1297–1300.

[32] Liu, S. Y.; Xue, D. S.; Li, J. H.; Wang, B. C.; Zang, Z. H.; Liao, M. X. Assay of Amino Acid in Cornu Caprae Hircus Extract. *Central South Pharm.* **2014**, *12*, 271–274.

[33] Liu, R.; Zhu, Z. H.; Qian, D. W.; Duan, J. A. Analysis and Identification of Proteins and Peptides from Goat. *Mass.* **2017**, *38*, 110–115.

[34] Upadhyay, R.; Mohan Rao, L. J. An Outlook on Chlorogenic Acids-Occurrence, Chemistry, Technology, and Biological Activities. *Crit. Rev. Food Sci. Nutr.* **2013**, *53*, 968–984. DOI: 10.1080/10408398.2011.576319.